



Thermodynamics of
sulfuric acid dimer
formation

A. Kürten et al.

This discussion paper is/has been under review for the journal Atmospheric Chemistry and Physics (ACP). Please refer to the corresponding final paper in ACP if available.

Thermodynamics of the formation of sulfuric acid dimers in the binary (H₂SO₄-H₂O) and ternary (H₂SO₄-H₂O-NH₃) system

A. Kürten¹, S. Münch¹, L. Rondo¹, F. Bianchi^{2,3}, J. Duplissy^{4,a}, T. Jokinen⁵, H. Junninen⁵, N. Sarnela⁵, S. Schobesberger^{5,b}, M. Simon¹, M. Sipilä⁵, J. Almeida⁴, A. Amorim⁶, J. Dommen², N. M. Donahue⁷, E. M. Dunne^{8,c}, R. C. Flagan⁹, A. Franchin⁵, J. Kirkby^{1,4}, A. Kupc¹⁰, V. Makhmutov¹¹, T. Petäjä⁵, A. P. Praplan^{2,5,d}, F. Riccobono^{2,e}, G. Steiner^{5,12,f}, A. Tomé⁶, G. Tsagkogeorgas¹³, P. E. Wagner¹⁰, D. Wimmer^{1,a}, U. Baltensperger², M. Kulmala⁵, D. R. Worsnop^{5,14}, and J. Curtius¹

¹Institute for Atmospheric and Environmental Sciences, Goethe-University Frankfurt am Main, Frankfurt am Main, Germany

²Laboratory of Atmospheric Chemistry, Paul Scherrer Institute, Villigen, Switzerland

³Institute for Atmospheric and Climate Science, ETH Zurich, Zurich, Switzerland

⁴CERN (European Organization for Nuclear Research), Geneva, Switzerland

⁵Department of Physics, University of Helsinki, Helsinki, Finland

Title Page	
Abstract	Introduction
Conclusions	References
Tables	Figures
◀	▶
◀	▶
Back	Close
Full Screen / Esc	
Printer-friendly Version	
Interactive Discussion	



Abstract

Sulfuric acid is an important gas influencing atmospheric new particle formation (NPF). Both the binary ($\text{H}_2\text{SO}_4\text{-H}_2\text{O}$) system, and the ternary system involving ammonia ($\text{H}_2\text{SO}_4\text{-H}_2\text{O-NH}_3$) may be important in the free troposphere. An essential step in the nucleation of aerosol particles from gas-phase precursors is the formation of a dimer, so an understanding of the thermodynamics of dimer formation over a wide range of atmospheric conditions is essential to describe NPF. We have used the CLOUD chamber to conduct nucleation experiments for these systems at temperatures from 208 to 248 K. Neutral monomer and dimer concentrations of sulfuric acid were measured using a Chemical Ionization Mass Spectrometer (CIMS). From these measurements dimer evaporation rates in the binary system were derived for temperatures of 208 and 223 K. We compare these results to literature data from a previous study that was conducted at higher temperatures but is in good agreement with the present study. For the ternary system the formation of $\text{H}_2\text{SO}_4 \bullet \text{NH}_3$ is very likely an essential step in the formation of sulfuric acid dimers, which were measured at 210, 223, and 248 K. We estimate the thermodynamic properties (dH and dS) of the $\text{H}_2\text{SO}_4 \bullet \text{NH}_3$ cluster using a simple heuristic model and the measured data. Furthermore, we report the first measurements of large neutral sulfuric acid clusters containing as many as 10 sulfuric acid molecules for the binary system using Chemical Ionization-Atmospheric Pressure interface-Time Of Flight (CI-API-TOF) mass spectrometry.

1 Introduction

The formation of new particles from the gas phase is a frequent and important process in the atmosphere. Substantial progress has been made in recent years describing the chemical systems and the mechanisms that could potentially be relevant to atmospheric new particle formation (NPF). Observed atmospheric boundary-layer nucleation rates typically correlate with the concentration of gaseous sulfuric acid (Kulmala

Thermodynamics of sulfuric acid dimer formation

A. Kürten et al.

Title Page

Abstract

Introduction

Conclusions

References

Tables

Figures



Back

Close

Full Screen / Esc

Printer-friendly Version

Interactive Discussion



Thermodynamics of sulfuric acid dimer formation

A. Kürten et al.

Title Page

Abstract

Introduction

Conclusions

References

Tables

Figures



Back

Close

Full Screen / Esc

Printer-friendly Version

Interactive Discussion



et al., 2004; Kuang et al., 2008). Moreover, it is generally accepted that the presence of water vapor enhances nucleation in the binary ($\text{H}_2\text{SO}_4\text{-H}_2\text{O}$) system. However, nucleation under typical ground-level conditions cannot be explained by the binary nucleation of sulfuric acid and water vapor (Kulmala et al., 2004; Kerminen et al., 2010), even if the enhancing effect due to ions is taken into account (Kirkby et al., 2011). Therefore, assuming that sulfuric acid is required for nucleation, at least one additional compound is necessary to stabilize the nucleating clusters (Zhang et al., 2012). Ammonia, amines and highly-oxidized organic compounds have been identified in ambient samples or tested in laboratory experiments (Ball et al., 1999; Hanson and Eisele, 2002; Chen et al., 2012; Kulmala et al., 2013). Recent chamber experiments showed that the observed atmospheric boundary layer nucleation rates can, in principle, be explained by sulfuric acid acting in combination with either amines or the oxidation products from α -pinene (Almeida et al., 2013; Schobesberger et al., 2013; Riccobono et al., 2014).

Nucleation has also frequently been observed in the free troposphere, where the temperature and gas mixture differ from those at the surface (Brock et al., 1995; Weber et al., 1995; Clarke et al., 1999; Lee et al., 2003). An important source for stratospheric particles is the tropical tropopause region where nucleation mode particles have been observed. Additionally, new particle formation has also been observed in the free troposphere (Brock et al., 1995; Clarke et al., 1999; Borrmann et al., 2010; Weigel et al., 2011). Due to the volatility and the identification of sulfur in collected particles it was concluded that binary nucleation contributes to (or dominates) the formation of these particles (Brock et al., 1995). Binary homogenous nucleation also seems to play an important role in forming the mid-stratospheric condensation nuclei layer, although ion-induced binary nucleation cannot be ruled-out (Campbell and Deshler, 2014). Several studies provide evidence that ion-induced nucleation may be an important process in the free troposphere (Lee et al., 2003; Lovejoy et al., 2004; Kanawade and Tripathi, 2006; Weigel et al., 2011). These studies suggest that binary nucleation is important on a global scale – especially in regions where very low temperatures prevail, and

where the concentrations of stabilizing substances involved in ternary nucleation are low.

Nucleation in the binary system starts with the collision of two hydrated sulfuric acid monomers, which form a dimer (Petäjä et al., 2011). In this study, the notation “dimer” refers to a cluster that contains two sulfuric acid molecules plus an unknown amount of water and, in the ternary system, ammonia. Similarly, the monomer of sulfuric acid may contain water or ammonia. Unless stated otherwise the terms “monomer” and “dimer” describe the neutral, i.e. uncharged molecules and clusters. The probability that a dimer will or will not grow larger depends on its evaporation rate as well as its collision rate with monomers and larger clusters. Therefore, it is crucial to know the evaporation rate (or the equilibrium constant) of the sulfuric acid dimer in order to understand and model binary nucleation. Hanson and Lovejoy (2006) measured the dimer equilibrium constant over a temperature range of 232 to 255 K. However, no direct measurements have been performed for lower temperatures. Moreover, evidence exists that ammonia is an important trace gas influencing new particle formation in some regions of the atmosphere (Weber et al., 1998; Chen et al., 2012). Numerous studies using quantum chemical calculations have been conducted to study the cluster thermodynamics for the sulfuric acid-ammonia system (Kurtén et al., 2007; Torpo et al., 2007; Ortega et al., 2012; Chon et al., 2014). To our knowledge, however, only very few studies have yet reported experimentally determined dimer concentrations for this system (Hanson and Eisele, 2002; Jen et al., 2014). In order to model NPF for the ternary system involving ammonia it is essential to better understand the thermodynamics of the clusters involved in the nucleation process from experiments in order to narrow down the uncertainties from the theoretical studies.

Here we present experimentally derived dimer evaporation rates for the binary system ($\text{H}_2\text{SO}_4\text{-H}_2\text{O}$) at temperatures of 208 and 223 K. The measurements of the sulfuric acid monomer and dimer were made with a Chemical Ionization Mass Spectrometer (CIMS) at the Cosmics Leaving OUTdoor Droplets (CLOUD) chamber. The data are discussed and compared to previously published dimer evaporation rates for the binary

Thermodynamics of sulfuric acid dimer formation

A. Kürten et al.

[Title Page](#)[Abstract](#)[Introduction](#)[Conclusions](#)[References](#)[Tables](#)[Figures](#)[Back](#)[Close](#)[Full Screen / Esc](#)[Printer-friendly Version](#)[Interactive Discussion](#)

Thermodynamics of sulfuric acid dimer formation

A. Kürten et al.

Title Page

Abstract

Introduction

Conclusions

References

Tables

Figures



Back

Close

Full Screen / Esc

Printer-friendly Version

Interactive Discussion



1.5 m times 1.5 m) using a defocused pion beam from CERN's proton synchrotron (Duplissy et al., 2010). Ultra-clean gas is provided to the chamber by mixing nitrogen and oxygen from cryogenic liquids at a ratio of 79 : 21. Different relative humidities (RH) can be achieved by passing a portion of the dry air through a nafion humidification system.

5 The temperature and the dew/frost point inside the chamber are monitored continuously; the RH is calculated using the equations given by Murphy and Koop (2005). A fibre optic system (Kupc et al., 2011) feeds UV light into the chamber, which initiates the photolytic production of sulfuric acid when H₂O, O₂, O₃, and SO₂ are present. Two mixing fans continuously stir the air inside the chamber assuring its homogeneity (Voigtländer et al., 2011).

10 The CLOUD5 campaign was dedicated to experiments investigating new particle formation at low temperatures (down to ~ 208 K) for the binary (H₂SO₄-H₂O) and the ternary (H₂SO₄-H₂O-NH₃) systems. The particle formation rates at low temperature will be reported in forthcoming papers; this publication focuses on measurement of the sulfuric acid monomer and the sulfuric acid dimer. One future paper will also focus on the determination of the ammonia mixing ratios at the low temperatures. These were evaluated from a careful characterization of the CLOUD gas system, which delivers ammonia diluted in ultra-clean nitrogen and air to the CLOUD chamber. The gas system was characterized by measurements with a Long Path Absorption Photometer (LOPAP, Bianchi et al., 2012), an Ion Chromatograph (IC, Praplan et al., 2012) and a Proton Transfer Reaction-Mass Spectrometer (PTR-MS, Norman et al., 2007).

2.2 Chemical Ionization Mass Spectrometer (CIMS) and Chemical Ionization-Atmospheric Pressure interface-Time Of Flight (CI-API-TOF) mass spectrometer

25 During CLOUD5 a Chemical Ionization Mass Spectrometer (CIMS) was used for the measurement of sulfuric acid monomers and dimers (Kürten et al., 2011). Using nitrate ions NO₃⁻ (HNO₃)_{x=0-2}, sulfuric acid can be selectively ionized; detection limits below

Thermodynamics of sulfuric acid dimer formation

A. Kürten et al.

Title Page

Abstract

Introduction

Conclusions

References

Tables

Figures



Back

Close

Full Screen / Esc

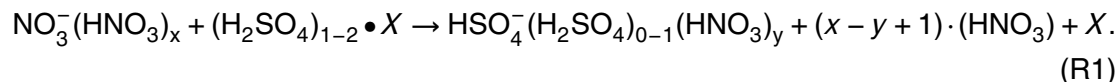
Printer-friendly Version

Interactive Discussion



10^5 cm^{-3} (referring to the monomer of sulfuric acid) can be reached for short integration times, thereby enabling high time resolution (Eisele and Tanner, 1993; Mauldin et al., 1999; Berresheim et al., 2000). The instrument was calibrated before and after the campaign using a system that produces a known concentration of sulfuric acid (Kürten et al., 2012). In this way, the recorded ion signals – for the primary ions and the reactant ions – can be converted into a concentration of sulfuric acid.

HSO_4^- (the product ion from the sulfuric acid monomer) and $\text{HSO}_4^-(\text{H}_2\text{SO}_4)$ (the product ion from the sulfuric acid dimer) are formed by reactions such as



The compound X is, in most cases, water, but in the case of the ternary system, both experiments and quantum chemical calculations suggest that dimers could also be bound to ammonia (Hanson and Eisele, 2002; Kurtén et al., 2007). Ammonia (or X) is expected to evaporate rapidly after the ionization (Ortega et al., 2014). It should be noted here that even if X did not evaporate after the ionization it would probably be removed in the CIMS collision dissociation chamber (CDC). In the CDC any remaining water molecules are stripped off from the core ions and the $\text{NO}_3^-(\text{HNO}_3)_{0-2}$ ions yield mostly NO_3^- due to the declustering. Therefore, the monomer and dimer sulfuric acid concentrations are estimated to be:

$$[\text{H}_2\text{SO}_4] = \frac{C}{L_{\text{monomer}}} \times \ln \left(1 + \frac{\text{CR}_{97}}{\text{CR}_{62}} \right), \quad (1a)$$

$$[(\text{H}_2\text{SO}_4)_2] = \frac{C}{L_{\text{dimer}}} \times \ln \left(1 + \frac{\text{CR}_{195}}{\text{CR}_{62}} \right). \quad (1b)$$

Here, CR denotes the count rate for the primary ions (CR_{62} at m/z 62 for NO_3^-), the HSO_4^- ions (CR_{97} at m/z 97) and the $\text{HSO}_4^-(\text{H}_2\text{SO}_4)$ ions (CR_{195} at m/z 195), respectively. The constant C is derived from a calibration and has been evaluated as

**Thermodynamics of
sulfuric acid dimer
formation**

A. Kürten et al.

Title Page

Abstract

Introduction

Conclusions

References

Tables

Figures



Back

Close

Full Screen / Esc

Printer-friendly Version

Interactive Discussion



$1.1 \times 10^{10} \text{ cm}^{-3}$ (Kürten et al., 2012). The same calibration constant is used for the monomer and the dimer because it is not possible to calibrate the dimer signal. Since both H_2SO_4 and $(\text{H}_2\text{SO}_4)_2$ are thought to react with the nitrate ions at the collision limit this assumption is well justified (the effect of transmission is discussed in Sect. 2.3).

The factors L_{monomer} and L_{dimer} take into account the penetration through the sampling line from the CLOUD chamber to the CIMS ion source. A sample flow rate of 7.6 standard liters per minute (slm) and a sampling line length of 100 cm were used to calculate the transmission. The diffusion coefficient has been calculated for the respective temperature and RH for the monomer from the data given by Hanson and Eisele (2000). It was assumed that the diffusivity of the dimer equals $0.06 \text{ cm}^2 \text{ s}^{-1}$ at 298 K, and varies with temperature as $(298 \text{ K}/T)^{1.75}$.

Some dimer dissociation in the CIMS CDC section cannot be ruled out, although the $\text{HSO}_4^-(\text{H}_2\text{SO}_4)$ ion has a very high bond energy (Curtius et al., 2001). However, as described in the next section, this effect is very likely minor, and, to the extent that it occurs, it is taken into account in the characterization of the dimer detection efficiency.

During the CLOUD7 campaign sulfuric acid and its clusters were measured with two Chemical Ionization-Atmospheric Pressure interface-Time Of Flight (CI-APi-TOF) mass spectrometers (Jokinen et al., 2012; Kürten et al., 2014); the H_2SO_4 monomer was also measured by the CIMS. However, during CLOUD7 it was not possible to measure the dimers with the CIMS due to instrumental problems. The CI-APi-TOF has an almost identical chemical ionization source as the CIMS but it uses a time of flight mass spectrometer with high mass resolution (around 4500 Th/Th) and mass accuracy (better than 10 ppm). These features as well as the wide mass range (up to around 2000 Th) enable detection and unambiguous identification of the elemental composition of clusters. As will be shown in Sect. 3.4 neutral clusters containing as many as 10 sulfuric acid molecules were detected during a binary experiment at 206 K.

2.3 Quantification of sulfuric acid dimer concentration

As it is not possible to calibrate the CIMS or the CI-APi-TOF with a known concentration of sulfuric acid dimers, a different method was chosen to allow the quantification of the dimer concentration. To estimate the relative sensitivity towards the dimers (m/z 195) in comparison to the monomer (m/z 97) ion-induced clustering (IIC) during calibration can be evaluated. If the sulfuric acid monomer concentration is large enough efficient formation of HSO_4^- (H_2SO_4) can occur due to clustering of HSO_4^- and H_2SO_4 within the CIMS ion drift tube (Hanson and Eisele, 2002). The estimated dimer count rate through this process is (Zhao et al., 2010; Chen et al., 2012)

$$\text{CR}_{195,\text{IIC}} = \frac{1}{2} \times k_{21} \times t_{\text{react}} \times \text{CR}_{97} \times C \times \ln \left(1 + \frac{\text{CR}_{97}}{\text{CR}_{62}} \right). \quad (2)$$

The reaction time t_{react} is approximately 50 ms in our case (Kürten et al., 2012). A value of $8 \times 10^{-10} \text{ cm}^3 \text{ s}^{-1}$ was used for k_{21} , the rate constant for reaction between HSO_4^- and H_2SO_4 (Zhao et al., 2010). The measured count rate CR_{195} was compared to the expected count rate during a calibration in which a high concentration of sulfuric acid monomers was presented to the CIMS. From this comparison, we concluded that the dimer signal is suppressed by a factor of 1.2 relative to the monomer signal. The discrepancy can either be due to mass discrimination or due to some fragmentation in the CIMS CDC. In any case, it means that the measured dimer signal needs to be multiplied by a factor of 1.2 (with an estimated statistical uncertainty of less than 10 %) when its concentration is evaluated.

The background signal, e.g., from electronic noise, is always subtracted before the dimer concentration is evaluated according to Eq. (1b). The background was obtained by averaging over a certain period just before the experiment started, i.e. before the UV lights were turned on and the H_2SO_4 was produced. In addition to the background, the contribution from IIC is subtracted from the dimer signal (Chen et al., 2012). This effect becomes relevant at about $1 \times 10^7 \text{ cm}^{-3}$ for the sulfuric acid monomer under the conditions of this study.

2.4 Sulfuric acid dimer evaporation rate

The goal of this study is to determine sulfuric acid dimer evaporation rates from data obtained by monomer and dimer measurements. In order to derive a formula for the evaporation rate it is useful to start with the basic equations governing the loss and the production of the clusters. Since low temperature conditions (208 and 223 K for the binary system) are considered in this study the assumption is made that only the smallest clusters (dimer and trimer) have appreciable evaporation rates (Hanson and Eisele, 2006). The balance equation for the dimer concentration in this case is

$$\frac{dN_2}{dt} = 0.5 \times G_{1,1} \times K_{1,1} \times N_1^2 + k_{3,e} \times N_3 - \left(k_{2,w} + k_{\text{dil}} + \sum_{i=1}^n G_{2,i} \times K_{2,i} \times N_i + k_{2,e} \right) \times N_2 \quad (3)$$

where N_i is the concentration of the cluster containing i sulfuric acid molecules, and $k_{i,e}$ is its evaporation rate. In a chamber experiment such as CLOUD, three loss processes are relevant for neutral particles; these include the wall loss rate $k_{i,w}$, the dilution rate k_{dil} through the replenishment of the chamber air (independent of particle size), and coagulation with the coefficient $K_{i,j}$ describing collisions between the clusters i and j . The factor $G_{i,j}$ represents an enhancement in the collision rates due to London–van-der-Waals forces (McMurry, 1980; Chan and Mozurkevich, 2001). In order to derive an expression for the dimer evaporation rate, we assume steady-state ($dN_2/dt = 0$). Equation (3) can then be written as

$$k_{2,e} = \frac{0.5 \times G_{1,1} \times K_{1,1} \times N_1^2}{N_2} + \frac{k_{3,e} \times N_3}{N_2} - \left(k_{2,w} + k_{\text{dil}} + \sum_{i=1}^n G_{2,i} \times K_{2,i} \times N_i \right). \quad (4)$$

It is useful to estimate the relative importance of the three terms on the right-hand side of Eq. (4). The numerator in the first term describes the production rate of dimers from monomers. The collision constant for two monomers is approximately $4 \times 10^{-10} \text{ cm}^3 \text{ s}^{-1}$. If the enhancement factor G due to London–van-der-Waals forces

[Title Page](#)[Abstract](#)[Introduction](#)[Conclusions](#)[References](#)[Tables](#)[Figures](#)[Back](#)[Close](#)[Full Screen / Esc](#)[Printer-friendly Version](#)[Interactive Discussion](#)

Thermodynamics of sulfuric acid dimer formation

A. Kürten et al.

Title Page

Abstract

Introduction

Conclusions

References

Tables

Figures

◀

▶

◀

▶

Back

Close

Full Screen / Esc

Printer-friendly Version

Interactive Discussion



is included, this value is $\sim 1 \times 10^{-9} \text{ cm}^3 \text{ s}^{-1}$ (McMurry, 1980; Chan and Mozurkevich, 2001). As an example, at 208 K under binary conditions, the smallest monomer concentration evaluated is $2 \times 10^6 \text{ cm}^{-3}$, at which point the dimer was evaluated as $1 \times 10^4 \text{ cm}^{-3}$ (Sect. 3.3). These values yield 0.2 s^{-1} for the first term. The second term is significantly smaller than the first term, so it can be neglected in the following discussion. The trimer concentration (although it was not measured) should be smaller than the dimer concentration because the trimer is produced from the dimer. Moreover, the trimer evaporation rate is expected to be lower than the dimer evaporation rate (e.g., $1.6 \times 10^{-3} \text{ s}^{-1}$ for the trimer, and 0.3 s^{-1} for the dimer at 208 K and 20 % RH, see Hanson and Lovejoy, 2006). The third term includes losses due to walls, dilution, and coagulation. The wall loss rate for a dimer is approximately $1.5 \times 10^{-3} \text{ s}^{-1}$, while loss due to dilution is $\sim 1 \times 10^{-4} \text{ s}^{-1}$ (Kürten et al., 2014). The loss due to coagulation depends on the particle size distribution, and can be important when the dimer evaporation rate is small. Loss of dimers due to collisions with monomers (i.e., growth to form trimers) then dominates the coagulation term, which is usually on the order of 10^{-2} s^{-1} (e.g. $N_1 = 1 \times 10^7 \text{ cm}^{-3}$ and $G_{1,1} \times K_{1,1} = 1 \times 10^{-9} \text{ cm}^3 \text{ s}^{-1}$). All elements of the third term are, thus, small compared with the first term, and so these can also be neglected. For the conditions of this study, consistent with the extrapolated data by Hanson and Lovejoy (2006), the evaporation rates are however larger than 10^{-2} s^{-1} . This means that evaporation dominates over the other losses; therefore, $k_{2,e}$ can be approximated by

$$k_{2,e} = \frac{0.5 \times G_{1,1} \times K_{1,1} \times N_1^2}{N_2}. \quad (5)$$

If losses by processes other than evaporation were not negligible, retrieval of evaporation rates would require use of a numeric model that also includes larger clusters since coagulation loss depends on concentrations of all other clusters. Nevertheless, model calculations simulating cluster and particle concentrations are needed to evaluate other effects relevant to this study, as will be discussed in the next sections.

**Thermodynamics of
sulfuric acid dimer
formation**

A. Kürten et al.

Title Page

Abstract

Introduction

Conclusions

References

Tables

Figures



Back

Close

Full Screen / Esc

Printer-friendly Version

Interactive Discussion



Comparison of the rate constants used for the reactions between HSO_4^- and H_2SO_4 (Sect. 2.3) and between H_2SO_4 and H_2SO_4 yields that the neutral-neutral collision rate is slightly faster than the charged-neutral collision rate. This is due to the relatively large enhancement factor from London–van-der-Waals forces for the neutral-neutral rates (McMurry, 1980; Chan and Mozurkevich, 2001) and the observation that the reaction between the bisulfate ion and sulfuric acid seems not to proceed at the collisional rate (Zhao et al., 2010).

2.5 SAWNUC model

The Sulfuric Acid Water NUCleation model (SAWNUC) of Lovejoy et al. (2004) simulates ion-induced nucleation in the binary system. Cluster growth is treated explicitly by a step-by-step addition of sulfuric acid molecules while equilibrium with water molecules is assumed due to the relatively high concentration of H_2O compared to $[\text{H}_2\text{SO}_4]$. SAWNUC takes into account sulfuric acid condensation and evaporation, coagulation, and losses due to walls and dilution (Ehrhart and Curtius, 2013). In SAWNUC, evaporation rates of small, negatively-charged clusters are based on measured thermodynamics (Lovejoy and Curtius, 2001; Froyd and Lovejoy, 2003). More detailed information on SAWNUC can be found in Lovejoy et al. (2004), Kazil and Lovejoy (2007), and Ehrhart and Curtius (2013).

As this study focuses on neutral binary nucleation, we neglect the charged-cluster channel, and only simulate the neutral channel. Coagulation coefficients have been calculated according to Chan and Mozurkevich (2001). They quantified London–van-der-Waals forces for particles in the binary system based on the theory by Sceats (1989). Within this study of nucleation at low temperatures, only dimer (and sometimes trimer) evaporation has been taken into account. The exact input parameters are specified in the following sections.

All model calculations have also been repeated using a numeric model recently presented by Kürten et al. (2014), which has been adapted to the binary system. The

results of the two independent models agree very well, which strengthens our confidence in the calculations that are presented below.

2.6 Dimer transmission through the sampling line

Previous dimer evaporation rates were evaluated with the CIMS ionization source integrated within a temperature-controlled flow tube (Hanson and Lovejoy, 2006). This set-up ensured that the temperature did not change between the times when the dimers were formed, and when they were ionized. In the present study, the dimers formed inside the CLOUD chamber, which is very precisely temperature-controlled. However, the monomers and dimers had to be transported from the chamber to the CIMS through a 100 cm long sampling line. The first ~ 80 cm of this line were held at the same temperature as the chamber because it protruded through the thermal housing and into the chamber. Moreover, the sampling line was enclosed by an insulated copper tube. Since a large part of the copper volume was placed inside the thermal housing, the cold temperature was maintained over the full length of the copper tube due to efficient heat conduction even for a short section of the tube that was located outside the chamber, while the insulation minimized heat transfer to the surrounding air. The CIMS ion drift tube was connected to the tip of the copper jacketed sampling line by means of a short tube that was not temperature-controlled, exposing the last 15 to 20 cm of the sampling line to warmer temperatures. In this region the dimers could in principle have suffered from evaporation.

To estimate the evaporation effect, a finite difference method was used to calculate the temperature profile, as well as the dimer concentration across the sampling line over its full length. Figure 1 shows the results for a chamber temperature of 223 K. The walls of the first 80 cm of the sampling line were held at 223 K, while the last 20 cm were held at 293 K (which was a typical maximum day-time temperature in the experimental hall during the CLOUD5 campaign). It should be noted that this is an extreme case because, in reality, the temperature would slowly approach 293 K over the last 20 cm due to heat conduction along the walls of the sampling line. However, the

Thermodynamics of sulfuric acid dimer formation

A. Kürten et al.

Title Page

Abstract

Introduction

Conclusions

References

Tables

Figures



Back

Close

Full Screen / Esc

Printer-friendly Version

Interactive Discussion



Thermodynamics of sulfuric acid dimer formation

A. Kürten et al.

Title Page

Abstract

Introduction

Conclusions

References

Tables

Figures



Back

Close

Full Screen / Esc

Printer-friendly Version

Interactive Discussion



calculations performed here are used to obtain an upper-bound estimate of the error due to evaporation. The temperature of the walls is indicated by the black color (223 K) and the grey color (293 K). Figure 1 shows the normalized concentration of dimers after initializing the monomer concentration to $1 \times 10^7 \text{ cm}^{-3}$; the dimer was assumed to be at equilibrium initially. It was further assumed that both monomers and dimers are lost to the walls due to diffusion, and that at the same time dimers are formed due to collisions of monomers, but can also evaporate. Larger clusters or particles were not taken into account. The dimer evaporation rate as a function of temperature was taken from the literature at this stage (Hanson and Lovejoy, 2006).

The profile shown in Fig. 1 indicates that, during the first 80 cm, dimers are lost primarily via diffusion because, in this section, they are essentially in equilibrium regarding formation and evaporation; only over the last 20 cm does evaporation have an appreciable effect on the dimer concentration. However, only the region close to the walls of the sampling line shows a rise in the gas temperature; the center of the sample flow is essentially unaffected. The estimated overall transmission efficiency for dimers is 0.228 at a flow rate of 7.6 slm in the half-inch tube (inner diameter ~ 10 mm). If the temperature were held constant at 223 K over the entire tube length, the transmission would increase to 0.475 because only wall losses would take place. Since the dimer concentration is corrected for the effect of diffusion loss (see Eq. 1b), the additional loss factor due to evaporation would be $(1/0.228)/(1/0.475) = 2.08$. However, this is an upper bound estimate of the error introduced through evaporation since the temperature is, in reality, gradually changing over the last 20 cm instead of increasing as a step function as simulated. For the lower temperature of 208 K, the effect is even smaller. From the estimations presented in this section it can, therefore be concluded that, while the sampling conditions are not ideal, the maximum error introduced is very likely smaller than a factor of 2 (see also error discussion in Sect. 3.7).

3 Results and discussion

3.1 Neutral vs. ion-induced experiments

Figure 2 (upper panel) shows the measured monomer and dimer concentrations from a binary experiment at 208 K. The experiment is started when the UV lights are turned on (at 14:16 UTC). The first stage is conducted in a neutral environment with the CFHV enabled. At 16:00 UTC (marked by the dashed vertical line) the electrodes are grounded and galactic cosmic rays (GCRs) lead to a build-up of ions in the chamber. While the monomer concentration is not affected by the GCRs, the dimer concentration is. For the neutral conditions the dimer signal above background is due to neutral $(\text{H}_2\text{SO}_4)_2$. During the GCR stage of the experiment, the dimer signal gradually increases. This could be due either to neutral dimers being charged in the CIMS or charged dimer ions forming within the CLOUD chamber.

Unfortunately, there was no ion filter installed in the CIMS sampling line during CLOUD5 to eliminate the ion contribution to the CIMS signal. However, evidence exists that the additional signal during GCR conditions is caused by a buildup of chamber ions rather than formation of additional neutral dimers during the ion-induced experiments. Recently, it was reported that HSO_4^- ions clustered to large oxidized organic molecules (OxOrg) can be efficiently detected by the CIMS (Rondo et al., 2014). Those experiments were conducted for the ternary system of sulfuric acid, water and pinanediol oxidation products at CLOUD. The most likely explanation for the signal enhancement seen by the CIMS is reduced sampling line loss of the clusters compared to HSO_4^- . This enhances the signal of HSO_4^- (which is not formed by ionization of neutral sulfuric acid in the CIMS drift tube). Upon reaching the CIMS CDC, the $\text{HSO}_4^- \bullet \text{OxOrg}$ clusters break apart, and the bisulfate ions are subsequently detected. This example shows that the CIMS can, in some cases, also be sensitive to ions and not just towards neutral molecules.

Thermodynamics of sulfuric acid dimer formation

A. Kürten et al.

Title Page

Abstract

Introduction

Conclusions

References

Tables

Figures



Back

Close

Full Screen / Esc

Printer-friendly Version

Interactive Discussion



Schobesberger et al., 2015). Our findings support the observation that the mixed sulfuric acid ammonia ion clusters are more stable than pure sulfuric acid clusters because they do not seem to fragment to the same extent. As a consequence of the observations discussed in this section, only neutral experiments were considered for the evaluation of the dimer evaporation rates in the binary system.

3.2 Effect of fragmentation during neutral experiments

In the binary system, large cluster ions can fragment and contribute to the measured dimer signal. In this section the maximum error due to the observed fragmentation described in Sect. 3.1 is estimated. For neutral cluster measurements, this process is, however, different from that described in the previous section. Under ion-induced conditions the ions are directly sampled from the CLOUD chamber. Therefore, a relatively low concentration of cluster ions can contribute significantly to the dimer signal because the ionization process in the CIMS drift tube is not needed for their detection.

In a worst-case scenario all cluster ions larger than the dimer (originating from neutral clusters after ionization) would fragment and yield one $\text{HSO}_4^- (\text{H}_2\text{SO}_4)$ thereby increasing the apparent dimer concentration. It is important to note that even a very large charged cluster could only yield one $\text{HSO}_4^- (\text{H}_2\text{SO}_4)$ because the clusters carry only one negative charge. The cluster concentrations (dimer and larger) can be calculated using the SAWNUC model. In any case, the cluster concentrations decrease with increasing size, so the potential contribution decreases with increasing cluster size. Figure 3 provides an upper bound estimate of the magnitude of this effect. In an example calculation for a temperature of 223 K, a sulfuric acid monomer concentration of $2 \times 10^7 \text{ cm}^{-3}$, and dimer and trimer evaporation rates from the literature (Hanson and Lovejoy, 2006) are used, while all other evaporation rates are set to zero. The model yields concentrations for the neutral dimer and all larger clusters. Integrating the concentrations from the dimer up to a certain cluster size, and normalizing the sum with the dimer concentration, yields the results shown in Fig. 3 which indicate that the contribution of the larger clusters to the dimer is, at most, a factor of 3 larger than that of

Thermodynamics of sulfuric acid dimer formation

A. Kürten et al.

Title Page

Abstract

Introduction

Conclusions

References

Tables

Figures



Back

Close

Full Screen / Esc

Printer-friendly Version

Interactive Discussion



Thermodynamics of sulfuric acid dimer formation

A. Kürten et al.

Title Page

Abstract

Introduction

Conclusions

References

Tables

Figures



Back

Close

Full Screen / Esc

Printer-friendly Version

Interactive Discussion



the dimers, even as one considers the contributions from very large clusters. Again, in this estimation it is considered that even a large fragmented cluster can contribute only one $\text{HSO}_4^-(\text{H}_2\text{SO}_4)$ because all clusters are singly charged. For this reason the cluster number concentrations are integrated and not the number of neutral dimers in a cluster.

The estimated factor in this section is an upper limit. It is unlikely that all clusters will fragment, or that they always yield $\text{HSO}_4^-(\text{H}_2\text{SO}_4)$ as the product. Instead, HSO_4^- might result from the fragmentation, because, not being an equilibrium process, fragmentation would not always yield the most stable cluster configuration. Moreover, since evaporation cools the cluster, evaporation of neutral sulfuric acid molecules from the largest clusters may be incomplete. In summary, the maximum effect of fragmentation is very likely on the order of a factor of 2, or lower (see also error discussion in Sect. 3.7).

3.3 Binary ($\text{H}_2\text{SO}_4\text{-H}_2\text{O}$) dimer concentrations and evaporation rates

Figure 4 shows the steady-state dimer concentrations as a function of the monomer concentrations at a temperature of 208 K. The data is segregated into binary neutral (solid circles) and ion-induced (open triangles). The color code indicates the relative humidity (RH) over ice. The black lines indicate the results from the SAWNUC model assuming four different dimer evaporation rates between 0 and 1 s^{-1} (indicated in the legend of the figure). Comparison between the modeled curves and the experimental data gives an indication of the magnitude of the dimer evaporation rates, but the actual values are calculated with Eq. (5) and will be discussed in the context of Fig. 6. While the model curves for 0.1 and 1 s^{-1} are straight lines with a slope of two on a log-log-plot, the lines for 0 and 0.01 s^{-1} show a pronounced curvature with a slope that approaches a value of one for the high monomer and dimer concentrations. This curvature indicates that a full model calculation would be required in order to derive even smaller evaporation rates than those observed in this study. If the evaporation rate is comparable to the other loss rates, these mechanisms need to be taken into account when estimat-

Thermodynamics of sulfuric acid dimer formation

A. Kürten et al.

Title Page

Abstract

Introduction

Conclusions

References

Tables

Figures

◀

▶

◀

▶

Back

Close

Full Screen / Esc

Printer-friendly Version

Interactive Discussion



ing $k_{2,e}$. Only when the evaporation rate dominates dimer loss over the full range of $[\text{H}_2\text{SO}_4]$ can other mechanisms be neglected. The neutral binary data in Fig. 4 indicate that the dimer evaporation rate varies between 0.2 s^{-1} for $\sim 20\%$ RH and 0.03 s^{-1} for 100% RH at 208 K . Therefore, relative humidity has a relatively strong effect, one that is more strongly pronounced than the higher temperature (232 to 255 K) data of Hanson and Lovejoy (2006) suggest (see discussion below). Our signal-to-noise ratio was, however, not high enough to quantify the dimer at temperatures above 223 K for direct comparison. Figure 4 also gives an idea of the magnitude of the ion effect on the CIMS dimer measurements (open triangles). As discussed in Sect. 3.1, the ion-induced binary experiments show systematically higher apparent dimer concentrations than do the neutral experiments. For this reason they are discarded when deriving dimer evaporation rates.

Figure 5 shows the monomer and dimer data for a temperature of 223 K . Again, the data show a pronounced influence of relative humidity. The dimer evaporation rate is approximately 7 s^{-1} at 20% RH and 0.5 s^{-1} at 80% RH. The ion enhancement effect can be divided into two regimes, one in which it seems to be limited by the availability of sulfuric acid, and a second one in which it is limited by the availability of ions and reaches a plateau where the dimer signal ceases to increase with the sulfuric acid monomer concentration (open triangles).

The evaporation rates derived herein can be compared with the rates reported by Hanson and Lovejoy (2006) after some unit conversions. The equilibrium constant K_{eq} for sulfuric acid dimer formation from monomers in the presence of water has been reported as (Hanson and Lovejoy, 2006)

$$K_{\text{eq}} = \frac{p_2}{(p_1)^2} = \frac{1}{\text{Pa}} \times \exp\left(\frac{A}{T} - B\right) \quad (6)$$

with $A = (9210 \pm 930) \text{ K}$, and $B = 31.4 \pm 3.9$ for the temperature, $232 \leq T \leq 255 \text{ K}$, and a relative humidity of 20% . Given the reported values for A and B the thermodynamic properties are estimated to be $dH = -18.3 \pm 1.8 \text{ kcal mol}^{-1}$ and $dS = -39.5 \pm$

Thermodynamics of sulfuric acid dimer formation

A. Kürten et al.

Title Page

Abstract

Introduction

Conclusions

References

Tables

Figures

◀

▶

◀

▶

Back

Close

Full Screen / Esc

Printer-friendly Version

Interactive Discussion



7.8 cal mol⁻¹ K⁻¹ (Hanson and Lovejoy, 2006). Equation (6) provides the equilibrium constant in units of Pa⁻¹ since the partial pressures p of the monomers and dimers are used. In order to calculate evaporation rates it is necessary to convert the equilibrium constant to units of cm³, and to further apply the relationship between equilibrium constant, evaporation rate, and collision constant for the dimers (Ortega et al., 2012), leading to:

$$k_e = 0.5 \cdot \frac{G_{1,1} \times K_{1,1}}{k_B \times T \times 10^6 \times K_{eq}}, \quad (7)$$

where k_B is the Boltzmann constant. We converted equilibrium constants reported by Hanson and Lovejoy (2006) to evaporation rates using Eq. (7), while the rates from this study are based on the data shown in Figs. 4 and 5 and Eq. (5). Figure 6 shows both data sets (triangles and circles). Fitting the combined data set for 20 % RH gives the following formulation for the equilibrium constant

$$K_{eq} = \frac{1}{Pa} \times \exp\left(\frac{(9371 \pm 649)K}{T} - (32.00 \pm 2.76)\right). \quad (8)$$

The solid black line in Fig. 6 shows the dimer evaporation rates derived from Eq. (8). The uncertainties in Eq. (8) are based on 95 % confidence intervals. Overall, the two data sets are consistent with one another, and yield $dH = -18.6 \pm 1.3$ kcal mol⁻¹ and $dS = -40.7 \pm 5.5$ cal mol⁻¹ K⁻¹. Hanson and Lovejoy (2006) reported that dimer evaporation rates decrease with increasing RH according to RH^p with $p = 0.5$, where the exponent p has an uncertainty of ± 100 %. Our data indicate a rather strong influence of RH on the evaporation rates, so we assumed an exponent of 1. The resulting dimer evaporation rates at 100 % RH are shown with a dashed line in Fig. 6. The high RH data at 208 K can very well be explained with the assumed dependency on the relative humidity.

3.4 Neutral cluster measurement with CI-API-TOF

During the CLOUD7 campaign, experiments were conducted at ~ 206 K under binary conditions. In addition to the CIMS two CI-API-TOFs were deployed (Jokinen et al., 2012; Kürten et al., 2014). The two instruments are labeled CI-API-TOF-UFRA (instrument from the University of Frankfurt) and CI-API-TOF-UHEL (instrument from the University of Helsinki). In contrast to the CIMS used during CLOUD5, the sampling lines of the CI-API-TOFs were not temperature-controlled. Therefore, dimer evaporation was likely more pronounced. For this reason, we did not attempt to quantify the dimer evaporation rate, although the dimer signals are quantitatively consistent with the data shown in Fig. 3. However, the CI-API-TOFs have a much wider mass range than the CIMS, i.e. a maximum of approximately 2000 Th. This increased mass range allowed larger clusters to be measured; indeed, neutral sulfuric acid clusters containing up to 10 sulfuric acid molecules, i.e. $\text{HSO}_4^-(\text{H}_2\text{SO}_4)_n$ (n from 0 to 9) were detected (Fig. 7). Eisele and Hanson (2000) previously reported detection of neutral clusters containing up to eight sulfuric acid molecules in a flow-tube experiment using a quadrupole mass spectrometer. Water molecules associated with the clusters were not detected with the CI-API-TOFs; these were most likely evaporated during ion transfer into the high vacuum section of the instruments. No ammonia was detected in any of the clusters either, even though ammonia can, in principle, be observed with a similar instrument that measures charged clusters (Kirkby et al., 2011), so it can be concluded that the experiment was, indeed, under pure binary conditions.

The upper panel of Fig. 7 shows the time-resolved signals from one of the CI-API-TOFs ranging from the monomer (HSO_4^- , i.e., S1) up to the decamer ($\text{HSO}_4^-(\text{H}_2\text{SO}_4)_9$, i.e., S10); all of these signals clearly increase following the start of the experiment at 10:02 UTC. From the time-resolved data, the steady-state signals for the different clusters were obtained for both instruments (red and blue circles in Fig. 7, lower panel). It was not attempted to derive concentrations from the count-rate signals due to the unknown influence of cluster evaporation within the sampling line and transmission within

Thermodynamics of sulfuric acid dimer formation

A. Kürten et al.

[Title Page](#)[Abstract](#)[Introduction](#)[Conclusions](#)[References](#)[Tables](#)[Figures](#)[Back](#)[Close](#)[Full Screen / Esc](#)[Printer-friendly Version](#)[Interactive Discussion](#)

the mass spectrometers. However, the CIMS, which was operated in parallel to the CI-APi-TOFs with its own dedicated sampling line, yielded a monomer concentration of $1.7 \times 10^7 \text{ cm}^{-3}$.

For this experiment we calculated the extent to which ion-induced clustering (IIC) could contribute to the signals. The equations provided by Chen et al. (2012) were used to estimate the maximum contribution from IIC (Fig. 7, lower panel). The dashed red line indicates what cluster signals would be expected if all neutral cluster concentrations (dimer and larger) were zero, and the only cluster ions were formed by addition of H_2SO_4 monomers to the HSO_4^- ions within the CIMS drift tube. The large discrepancy between the observations (red circles) and the dashed red line (it falls off very steeply with increasing cluster size) shows that the contribution from IIC is negligible. Using SAWNUC together with the dimer and trimer evaporation rates (from this study and from Hanson and Lovejoy (2006), respectively) allows us to predict all cluster concentrations and then calculate the expected signals (black curve). While the expected signals from the model calculation are substantially higher than the measured ones from the CI-APi-TOF-UFRA, the shape of the black (modeled) and the red (measured) curve is very similar. This is consistent with the assumption that cluster evaporation rates are negligible for the trimers and all larger clusters at this low temperature. The slightly steeper slope of the measurements could be due to a decrease in the detection efficiency as a function of mass of the CI-APi-TOF-UFRA. In this context it is also important to note that the CI-APi-TOF-UFRA was tuned differently than in a previous study (Kürten et al., 2014) in which a relatively steep drop in the sensitivity as a function of mass was observed. The tuning in this study might have led to a more constant detection efficiency as a function of mass. The fact that the measured trimer signal is lower than the tetramer signal is thought to result from fragmentation of the trimers. Similarly, the hexamer appears to suffer some fragmentation. The CI-APi-TOF-UHEL was tuned to maximize the signals in the mass range up to the pentamer. Consequently, in comparison to the other CI-APi-TOF, this led to substantially higher signals in the mass region up to the pentamer, with a pronounced local maximum around the tetramer (blue

Thermodynamics of sulfuric acid dimer formation

A. Kürten et al.

Title Page

Abstract

Introduction

Conclusions

References

Tables

Figures



Back

Close

Full Screen / Esc

Printer-friendly Version

Interactive Discussion



curve in Fig. 7). However, for the larger masses the signal drops, reaching levels that are comparable to those from the CI-API-TOF-UFRA.

Because so many questions remain regarding fragmentation, cluster quantification, and the effect of evaporation in the sampling line, the CI-API-TOF signals are only discussed qualitatively in the present study.

3.5 Sulfuric acid dimer concentrations in the ternary ($\text{H}_2\text{SO}_4\text{-H}_2\text{O-NH}_3$) system

During CLOUD5, ternary nucleation experiments were conducted at temperatures of 210, 223, and 248 K. The addition of relatively small amounts of ammonia (mixing ratios below ~ 10 pptv) led to a significant increase in the sulfuric acid dimer concentrations compared to the binary system confirming the enhancing effect of ammonia on new particle formation (Ball et al., 1999; Kirkby et al., 2011; Zollner et al., 2012; Jen et al., 2014). In the presence of NH_3 , a fraction of the sulfuric acid will be bound to ammonia. However, we assume that the sulfuric acid monomers and dimers will still be ionized by the nitrate primary ions at the same rate as the pure compounds. The ammonia will, however, evaporate very rapidly after the ionization (Hanson and Eisele, 2002). For this reason it is not possible to determine directly the fractions of either the sulfuric acid monomer or the dimer that contain ammonia. Therefore, in the following we assume that the measured monomer is the sum of the pure sulfuric acid monomer and the sulfuric acid monomer bound to ammonia; the same assumption is made for the dimer.

Figure 8 shows the measured sulfuric acid dimer concentration as a function of the sulfuric acid monomer concentration for three different temperatures (210, 223, and 248 K), and several ammonia mixing ratios ($< \sim 10$ pptv) under ternary conditions. Two limiting cases that bracket the possible dimer concentrations and the influence of ammonia are indicated by the solid black line and the dashed black line. The solid black line shows the case in which all evaporation rates are set to zero in the SAWNUC model (the kinetic limit); the dashed black line indicates the case for binary conditions at 40 % RH. It can be seen that, at the lowest temperature (210 K), the dimer concentrations

Thermodynamics of sulfuric acid dimer formation

A. Kürten et al.

Title Page

Abstract

Introduction

Conclusions

References

Tables

Figures



Back

Close

Full Screen / Esc

Printer-friendly Version

Interactive Discussion



are close to the expected concentrations for kinetically limited cluster formation, as has been previously reported for the ternary sulfuric acid, water and dimethylamine system at 278 K (Kürten et al., 2014). The ammonia mixing ratio is ~ 7 pptv in this case (Fig. 8, upper panel). At 223 K two different ammonia mixing ratios were investigated.

It can clearly be seen that the dimer concentrations increase with increasing ammonia mixing ratio. Different ammonia mixing ratios (~ 2.5 to 8 pptv) were also studied at 248 K, but in this case the variation in the ammonia concentration was smaller than for 223 K; therefore, the dimer concentration variation is also less pronounced. In addition, the relative humidity changed from experiment to experiment (RH is indicated by the small numbers written next to the data points); it apparently influenced the dimer concentration, which is not surprising given the results described in Sect. 3.3, and those of Hanson and Lovejoy (2006). Our data show that very small ammonia mixing ratios (pptv range) can strongly enhance dimer formation under atmospherically relevant sulfuric acid concentrations and low temperatures.

3.6 Thermodynamics of the $\text{H}_2\text{SO}_4 \bullet \text{NH}_3$ cluster

In order to better understand what influences the dimer concentration in the ternary system, we have developed a simple model (Fig. 9); this is motivated by recent studies of acid-base nucleation of sulfuric acid, ammonia, and amines (Chen et al., 2012; Paasonen et al., 2012; Jen et al., 2014). Following the notation of Chen et al. (2012), a sulfuric acid molecule is termed A , while the base ammonia is termed B . Dimers (A_2 or A_2B) may form via two different routes: (a) two sulfuric acid molecules A can collide and form a pure sulfuric acid dimer (A_2), which can further collide with B and form A_2B , or (b) a sulfuric acid molecule can collide with an ammonia molecule and form an AB cluster, which can further collide with A (or another AB cluster) to form A_2B (or A_2B_2). The model further assumes that trimers can either contain solely sulfuric acid (A_3), or are associated with ammonia (A_3B_x).

For all larger clusters we make no distinction between pure sulfuric acid clusters and ammonia containing clusters. We further assume that the clusters cannot contain

Thermodynamics of sulfuric acid dimer formation

A. Kürten et al.

Title Page

Abstract

Introduction

Conclusions

References

Tables

Figures



Back

Close

Full Screen / Esc

Printer-friendly Version

Interactive Discussion



dimer concentration matched the measured one under steady-state conditions. From the evaporation rates at the different temperatures the thermodynamics (dH and dS) of the cluster AB were retrieved from a least-square linear fit (logarithm of the equilibrium constant vs. the inverse temperature) which yields $dH = -16.07 \text{ kcal mol}^{-1}$ and $dS = -26.24 \text{ cal mol}^{-1} \text{ K}^{-1}$ for $\text{H}_2\text{SO}_4 \bullet \text{NH}_3$.

Unfortunately, the number of data points used to derive the dH and dS values is quite small. At 210 K the measured dimer concentrations are very close to the kinetic limit estimation, so the evaporation rates must be very low. This indicates that small variations in the monomer and dimer concentration can lead to a large variation in the evaporation rate of AB . These data points were, therefore, neglected. On the other hand, the effect of the relative humidity on the evaporation rates of ammonia containing clusters is not known, so only those experiments that were conducted at similar RH, i.e., $\sim 36\%$, were considered.

Figure 8 also shows the calculated dimer concentrations using the model with the evaporation rate of AB inferred using the derived thermodynamics (open colored triangles). The error bars reflect a variation of the evaporation rate for $\text{H}_2\text{SO}_4 \bullet \text{NH}_3$ by a factor of 5 and 0.2. The good agreement between measured and modeled values indicates that the model successfully describes dimer concentrations over a wide range of conditions. We have also simulated the experiments of Hanson and Eisele (2002) for the ternary system involving ammonia, who used a sulfuric acid concentration of $1.9 \times 10^9 \text{ cm}^{-3}$ and an ammonia concentration of $3.8 \times 10^9 \text{ cm}^{-3}$ at a temperature of 265 K and an RH of $\sim 10\%$. Our calculated dimer concentration agrees with their measured concentration within better than a factor of two.

Table 1 compares our dH and dS values as well as the corresponding evaporation rates for selected temperatures with other data mainly obtained from quantum chemical calculations (Torpo et al., 2007; Ortega et al., 2012; Chon et al., 2014; Jen et al., 2014). Overall, the agreement is good, although the uncertainty of our values is quite high. However, it is difficult to derive an error estimate due to the small number of data points. One needs to keep in mind that the cluster formation was observed at $\sim 36\%$

Thermodynamics of sulfuric acid dimer formation

A. Kürten et al.

Title Page

Abstract

Introduction

Conclusions

References

Tables

Figures



Back

Close

Full Screen / Esc

Printer-friendly Version

Interactive Discussion



RH in this study, while the theoretical studies did not take into account the effect of water. The comparison in Table 1 also lists the experimental study by Jen et al. (2014) who determined the evaporation rate of $\text{H}_2\text{SO}_4 \bullet \text{NH}_3$ at ~ 300 K from a transient version of their second scheme (formation of dimers only via AB , see above). The extrapolated value from the present study is, however, in relatively good agreement with their value. The somewhat lower evaporation rate of Jen et al. (2014) could be explained by the fact that they did not consider the formation of dimers by self-coagulation of A . Furthermore, they assumed that the trimer has an evaporation rate of 0.4 s^{-1} . Both these assumptions require a slower evaporation rate for AB than our study suggests to explain the measured dimer concentrations at a given monomer and base concentration.

Overall, our measurements in the ternary system yield values of the thermodynamic properties of the $\text{H}_2\text{SO}_4 \bullet \text{NH}_3$ cluster that are in good agreement with the results from quantum chemical calculations. However, since the number of data points is limited, the uncertainty is rather high. Nevertheless, it seems that, within the accuracy of the measurements, the evaporation rates for $\text{H}_2\text{SO}_4 \bullet \text{NH}_3$ from both quantum chemistry and the present study are appropriate for use in nucleation models.

3.7 Uncertainties

The error bars shown in Figs. 4 and 5 include the standard variation of the individual data points and a 30 % (50 %) uncertainty in the monomer (dimer) concentration. The two error components are added together in quadrature. The systematic errors are estimated based on the uncertainties in the calibration coefficient C and the sampling line transmission. The error bars in Fig. 6 are obtained when using Gaussian error propagation on Eq. (5) for the monomer and the dimer concentration.

In addition to these errors, the effects of evaporation of the dimer in the sampling line (Sect. 2.6) and fragmentation (Sect. 3.2) have been discussed above. Each of these effects is very likely on the order of a factor of two or smaller. These processes probably influence all of the dimer data to some extent. However, these errors work in opposite directions: evaporation will lead to a reduction of the dimer concentration,

while fragmentation of larger clusters will tend to increase the apparent concentration. Therefore, the two effects partially compensate each other, so they were not taken into account in the calculation of the error bars.

One additional uncertainty is introduced by the assumption that the CIMS detection efficiency is independent of temperature. The study of Viggiano et al. (1997) indicates that the collision rate between nitrate primary ions and sulfuric acid is only a weak function of temperature between 200 and 300 K. Therefore, we expect that temperature only has a small effect on the sulfuric acid concentrations.

The estimates of the thermodynamic properties of the $\text{H}_2\text{SO}_4 \bullet \text{NH}_3$ cluster also rely on the assumptions made in the model (Sect. 3.6). One of the important assumptions made is that the base-containing trimer and tetramer do not evaporate significantly. The data of Ortega et al. (2012) suggest that the evaporation rates of the A_3B_1 and the A_4B_1 clusters are not negligible, even at temperatures at and below 248 K. In contrast, the base containing dimer (A_2B) has a very small evaporation rate. No experimental data have been found that support the relatively high evaporation rates of the base containing trimer and tetramer. Instead, the study by Hanson and Eisele (2002) concluded that the critical cluster in the $\text{H}_2\text{SO}_4\text{-H}_2\text{O-NH}_3$ system very likely contains two sulfuric acid molecules and one ammonia molecule at temperatures up to 275 K. In addition, an evaporation rate of 0.4 s^{-1} for the base-containing trimer could explain observed atmospheric nucleation rates at relatively warm temperatures of 300 K (Chen et al., 2012). This evaporation rate should decrease further at lower temperatures. Significant uncertainties remain regarding the evaporation rates of these clusters; further experiments will be needed to reduce these in the future.

4 Summary and conclusions

A Chemical Ionization Mass Spectrometer (CIMS) was used to measure the concentrations of the neutral sulfuric acid monomer and dimer during nucleation experiments at the CLOUD chamber. These experiments were conducted at temperatures as low

Thermodynamics of sulfuric acid dimer formation

A. Kürten et al.

Title Page

Abstract

Introduction

Conclusions

References

Tables

Figures



Back

Close

Full Screen / Esc

Printer-friendly Version

Interactive Discussion



as 208 K, making them relevant to conditions in the free troposphere. Both, the binary ($\text{H}_2\text{SO}_4\text{-H}_2\text{O}$) system, and the ternary system involving ammonia ($\text{H}_2\text{SO}_4\text{-H}_2\text{O-NH}_3$) were investigated.

Comparison of neutral and ion-induced nucleation experiments indicate that the CIMS detected a significant number of fragmented ion clusters. This confirms the so called “ion-effect” on the CIMS measurements that was recently described by Rondo et al. (2014). However, while Rondo et al. (2014) observed that fragmented $\text{HSO}_4^- \bullet \text{OxOrg}$ clusters contributed to the CIMS sulfuric acid monomer measurement, we observed a similar effect for the CIMS sulfuric acid dimer measurement (m/z 195). Interestingly, the ion effect on the CIMS dimers was almost absent as soon as ammonia was present in the CLOUD chamber. This is consistent with the observation that ammonia stabilizes sulfuric acid clusters and, thereby, enhances nucleation (Kirkby et al., 2011; Schobesberger et al., 2015).

From the measured monomer and dimer signals dimer evaporation rates were derived and compared to previous flow tube measurements made by Hanson and Lovejoy (2006) for the binary system. Their measurements were performed over a temperature range of 232 to 255 K. The data from the present study were obtained at lower temperatures, 208 to 223 K. Together, the two data sets yield a slightly revised version of the Hanson and Lovejoy (2006) formulation for the dimer equilibrium constant at 20 % RH with $dH = -18.6 \pm 1.3 \text{ kcal mol}^{-1}$ and $dS = -40.7 \pm 5.5 \text{ cal mol}^{-1} \text{ K}^{-1}$. Due to the wide temperature range (208 to 255 K) covered by the two data sets, this new estimate provides a high degree of confidence when being used at the very low temperatures where binary nucleation can be efficient. Regarding the formation of dimers in the binary system Hanson and Lovejoy (2006) stated that an increase in the relative humidity leads to an increase in the dimer equilibrium constant ($K_p \sim \text{RH}^p$) with a power dependency of p between 0 and 1. The best estimate for the power dependency was reported to be 0.5 (Hanson and Lovejoy, 2006). Our data indicate that the exponent is close to 1, i.e., at the upper end of what has been previously assumed.

Thermodynamics of sulfuric acid dimer formation

A. Kürten et al.

Title Page

Abstract

Introduction

Conclusions

References

Tables

Figures



Back

Close

Full Screen / Esc

Printer-friendly Version

Interactive Discussion



that observation of nucleating clusters in the atmosphere should be feasible. In the future, aircraft operation or measurements at high-altitude stations using CI-API-TOF could provide insight into the importance of binary vs. ternary ammonia nucleation in the free troposphere.

5 *Acknowledgements.* We would like to thank CERN for supporting CLOUD with important technical and financial resources, and for providing a particle beam from the CERN Proton Synchrotron. This research was funded by the European Commission Seventh Framework Programme (Marie Curie Initial Training Network “CLOUD-ITN”, grant no. 215 072), the German Federal Ministry of Education and Research (project nos. 01LK0902A and 01LK1222A), the European Research Council Advanced Grant “ATMNUCLE” (project no. 227 463), the Academy of Finland (project nos. 1 133 872, 1 118 615, and 272 041), the Swiss National Science Foundation (project nos. 200 020_135 307 and 206 620_141 278), the US National Science Foundation (grants AGS-1 439 551 and AGS-1 447 056), the Austrian Science Fund (project nos. P19546 and L593), and the Davidow foundation. We thank the tofTools team for providing tools for mass spectrometry analysis.

References

Almeida, J., Schobesberger, S., Kürten, A., Ortega, I. K., Kupiainen-Määttä, O., Praplan, A. P., Adamov, A., Amorim, A., Bianchi, F., Breitenlechner, M., David, A., Dommen, J., Donahue, N. M., Downard, A., Dunne, E. M., Duplissy, J., Ehrhart, S., Flagan, R. C., Franchin, A., Guida, R., Hakala, J., Hansel, A., Heinritzi, M., Henschel, H., Jokinen, T., Junninen, H., Kajos, M., Kangasluoma, J., Keskinen, H., Kupc, A., Kurtén, T., Kvashin, A. N., Laaksonen, A., Lehtipalo, K., Leiminger, M., Leppä, J., Loukonen, V., Makhmutov, V., Mathot, S., McGrath, M. J., Nieminen, T., Olenius, T., Onnela, A., Petäjä, T., Riccobono, F., Riipinen, I., Rissanen, M., Rondo, L., Ruuskanen, T., Santos, F. D., Sarnela, N., Schallhart, S., Schnitzhofer, R., Seinfeld, J. H., Simon, M., Sipilä, M., Stozhkov, Y., Stratmann, F., Tomé, A., Tröstl, J., Tsagkogeorgas, G., Vaattovaara, P., Viisanen, Y., Virtanen, A., Vrtala, A., Wagner, P. E., Weingartner, E., Wex, H., Williamson, C., Wimmer, D., Ye, P., Yli-Juuti, T., Carslaw, K. S., Kulmala, M., Curtius, J., Baltensperger, U., Worsnop, D. R., Vehkamäki, H.,

Thermodynamics of sulfuric acid dimer formation

A. Kürten et al.

Title Page

Abstract

Introduction

Conclusions

References

Tables

Figures



Back

Close

Full Screen / Esc

Printer-friendly Version

Interactive Discussion



**Thermodynamics of
sulfuric acid dimer
formation**

A. Kürten et al.

Title Page

Abstract

Introduction

Conclusions

References

Tables

Figures



Back

Close

Full Screen / Esc

Printer-friendly Version

Interactive Discussion



and Kirkby, J.: Molecular understanding of sulphuric acid-amine particle nucleation in the atmosphere, *Nature*, 502, 359–363, 2013.

Ball, S. M., Hanson, D. R., Eisele, F. L., and McMurry, P. H.: Laboratory studies of particle nucleation: initial results for H₂SO₄, H₂O, and NH₃ vapors, *J. Geophys. Res.*, 104, 23709–23718, doi:10.1029/1999JD900411, 1999.

Berresheim, H., Elste, T., Plass-Dülmer, C., Eisele, F. L., and Tanner, D. J.: Chemical ionization mass spectrometer for long-term measurements of atmospheric OH and H₂SO₄, *Int. J. Mass Spectrom.*, 202, 91–109, 2000.

Bianchi, F., Dommen, J., Mathot, S., and Baltensperger, U.: On-line determination of ammonia at low pptv mixing ratios in the CLOUD chamber, *Atmos. Meas. Tech.*, 5, 1719–1725, doi:10.5194/amt-5-1719-2012, 2012.

Borrmann, S., Kunkel, D., Weigel, R., Minikin, A., Deshler, T., Wilson, J. C., Curtius, J., Volk, C. M., Homan, C. D., Ulanovsky, A., Ravegnani, F., Viciani, S., Shur, G. N., Belyaev, G. V., Law, K. S., and Cairo, F.: Aerosols in the tropical and subtropical UT/LS: in-situ measurements of submicron particle abundance and volatility, *Atmos. Chem. Phys.*, 10, 5573–5592, doi:10.5194/acp-10-5573-2010, 2010.

Brock, C. A., Hamill, P., Wilson, J. C., Jonsson, H. H., and Chan, K. R.: Particle formation in the upper tropical troposphere: a source of nuclei for the stratospheric aerosol, *Science*, 270, 1650–1653, 1995.

Campbell, P. and Deshler, T.: Condensation nuclei measurements in the midlatitude (1982–2012) and Antarctic (1986–2010) stratosphere between 20 and 35 km, *J. Geophys. Res.*, 119, 137–152, doi:10.1002/2013JD019710, 2014.

Chan, T. W. and Mozurkewich, M.: Measurement of the coagulation rate constant for sulfuric acid particles as a function of particle size using tandem differential mobility analysis, *J. Aerosol Sci.*, 32, 321–339, 2001.

Chen, M., Titcombe, M., Jiang, J., Jen, C., Kuang, C., Fischer, M. L., Eisele, F. L., Siepmann, J. I., Hanson, D. R., Zhao, J., and McMurry, P. H.: Acid–base chemical reaction model for nucleation rates in the polluted atmospheric boundary layer, *P. Natl. Acad. Sci. USA*, 109, 18713–18718, doi:10.1073/pnas.1210285109, 2012.

Chon, N. L., Lee, S.-H., and Lin, H.: A theoretical study of temperature dependence of cluster formation from sulfuric acid and ammonia, *Chem. Phys.*, 433, 60–66, 2014.

**Thermodynamics of
sulfuric acid dimer
formation**

A. Kürten et al.

Title Page

Abstract

Introduction

Conclusions

References

Tables

Figures



Back

Close

Full Screen / Esc

Printer-friendly Version

Interactive Discussion



- Clarke, A. D., Eisele, F., Kapustin, V. N., Moore, K., Tanner, D., Mauldin, L., Litchy, M., Lienert, B., Carroll, M. A., and Albercook, G.: Nucleation in the equatorial free troposphere: favorable environments during PEM-Tropics, *J. Geophys. Res.*, 104, 5735–5744, 1999.
- 5 Curtius, J., Froyd, K. D., and Lovejoy, E. R.: Cluster ion thermal decomposition (I): experimental kinetics study and ab initio calculations for $\text{HSO}_4^- (\text{H}_2\text{SO}_4)_x (\text{HNO}_3)_y$, *J. Phys. Chem. A*, 105, 10867–10873, 2001.
- Duplissy, J., Enghoff, M. B., Aplin, K. L., Arnold, F., Aufmhoff, H., Avngaard, M., Baltensperger, U., Bondo, T., Bingham, R., Carslaw, K., Curtius, J., David, A., Fastrup, B., Gagné, S., Hahn, F., Harrison, R. G., Kellelt, B., Kirkby, J., Kulmala, M., Laakso, L., Laakso-
- 10 nen, A., Lillestol, E., Lockwood, M., Mäkelä, J., Makhmutov, V., Marsh, N. D., Nieminen, T., Onnela, A., Pedersen, E., Pedersen, J. O. P., Polny, J., Reichl, U., Seinfeld, J. H., Sipilä, M., Stozhkov, Y., Stratmann, F., Svensmark, H., Svensmark, J., Veenhof, R., Verheggen, B., Viisanen, Y., Wagner, P. E., Wehrle, G., Weingartner, E., Wex, H., Wilhelmsson, M., and Winkler, P. M.: Results from the CERN pilot CLOUD experiment, *Atmos. Chem. Phys.*, 10, 1635–1647, doi:10.5194/acp-10-1635-2010, 2010.
- Ehrhart, S. and Curtius, J.: Influence of aerosol lifetime on the interpretation of nucleation experiments with respect to the first nucleation theorem, *Atmos. Chem. Phys.*, 13, 11465–11471, doi:10.5194/acp-13-11465-2013, 2013.
- Eisele, F. L. and Hanson, D. R.: First measurement of prenucleation molecular clusters, *J. Phys. Chem. A*, 104, 830–836, 2000.
- 20 Eisele, F. L. and Tanner, D. J.: Measurement of the gas phase concentration of H_2SO_4 and methane sulfonic acid and estimates of H_2SO_4 production and loss in the atmosphere, *J. Geophys. Res.*, 98, 9001–9010, 1993.
- Eisele, F. L., Lovejoy, E. R., Kosciuch, E., Moore, K. F., Mauldin III, R. L., Smith, J. N., McMurry, P. H., and Iida, K.: Negative atmospheric ions and their potential role in ion-induced nucleation, *J. Geophys. Res.*, 111, D04305, doi:10.1029/2005JD006568, 2006.
- 25 Froyd, K. D. and Lovejoy, E. R.: Experimental thermodynamics of cluster ions composed of H_2SO_4 and H_2O , 2. Measurements and ab initio structures of negative ions, *J. Phys. Chem. A*, 107, 9812–9824, 2003.
- 30 Hanson, D. R. and Eisele, F.: Diffusion of H_2SO_4 in humidified nitrogen: hydrated H_2SO_4 , *J. Phys. Chem. A*, 104, 1715–1719, 2000.
- Hanson, D. R. and Eisele, F. L.: Measurement of prenucleation molecular clusters in the NH_3 , H_2SO_4 , H_2O system, *J. Geophys. Res.*, 107, 4158, doi:10.1029/2001JD001100, 2002.

Thermodynamics of sulfuric acid dimer formation

A. Kürten et al.

Title Page

Abstract

Introduction

Conclusions

References

Tables

Figures



Back

Close

Full Screen / Esc

Printer-friendly Version

Interactive Discussion



- Hanson, D. R. and Lovejoy, E. R.: Measurement of the thermodynamics of the hydrated dimer and trimer of sulfuric acid, *J. Phys. Chem. A*, 110, 9525–9528, 2006.
- Jen, C., McMurry, P. H., and Hanson, D. R.: Stabilization of sulfuric acid dimers by ammonia, methylamine, dimethylamine, and trimethylamine, *J. Geophys. Res.-Atmos.*, 119, 7502–7514, doi:10.1002/2014JD021592, 2014.
- Jokinen, T., Sipilä, M., Junninen, H., Ehn, M., Lönn, G., Hakala, J., Petäjä, T., Mauldin III, R. L., Kulmala, M., and Worsnop, D. R.: Atmospheric sulphuric acid and neutral cluster measurements using CI-API-TOF, *Atmos. Chem. Phys.*, 12, 4117–4125, doi:10.5194/acp-12-4117-2012, 2012.
- Junninen, H., Ehn, M., Petäjä, T., Luosujärvi, L., Kotiaho, T., Kostianen, R., Rohner, U., Gonnin, M., Fuhrer, K., Kulmala, M., and Worsnop, D. R.: A high-resolution mass spectrometer to measure atmospheric ion composition, *Atmos. Meas. Tech.*, 3, 1039–1053, doi:10.5194/amt-3-1039-2010, 2010.
- Kanawade, V. and Tripathi, S. N.: Evidence for the role of ion-induced particle formation during an atmospheric nucleation event observed in Tropospheric Ozone Production about the Spring Equinox (TOPSE), *J. Geophys. Res.*, 111, D02209, doi:10.1029/2005JD006366, 2006.
- Kazil, J. and Lovejoy, E. R.: A semi-analytical method for calculating rates of new sulfate aerosol formation from the gas phase, *Atmos. Chem. Phys.*, 7, 3447–3459, doi:10.5194/acp-7-3447-2007, 2007.
- Kerminen, V.-M., Petäjä, T., Manninen, H. E., Paasonen, P., Nieminen, T., Sipilä, M., Junninen, H., Ehn, M., Gagné, S., Laakso, L., Riipinen, I., Vehkamäki, H., Kurten, T., Ortega, I. K., Dal Maso, M., Brus, D., Hyvärinen, A., Lihavainen, H., Leppä, J., Lehtinen, K. E. J., Mirme, A., Mirme, S., Hörrak, U., Berndt, T., Stratmann, F., Birmili, W., Wiedensohler, A., Metzger, A., Dommen, J., Baltensperger, U., Kiendler-Scharr, A., Mentel, T. F., Wildt, J., Winkler, P. M., Wagner, P. E., Petzold, A., Minikin, A., Plass-Dülmer, C., Pöschl, U., Laaksonen, A., and Kulmala, M.: Atmospheric nucleation: highlights of the EUCAARI project and future directions, *Atmos. Chem. Phys.*, 10, 10829–10848, doi:10.5194/acp-10-10829-2010, 2010.
- Kirkby, J., Curtius, J., Almeida, J., Dunne, E., Duplissy, J., Ehrhart, S., Franchin, A., Gagné, S., Ickes, L., Kürten, A., Kupc, A., Metzger, A., Riccobono, F., Rondo, L., Schobesberger, S., Tsagkogeorgas, G., Wimmer, D., Amorim, A., Bianchi, F., Breitenlechner, M., David, A., Dommen, J., Downard, A., Ehn, M., Flagan, R. C., Haider, S., Hansel, A., Hauser, D., Jud, W., Junninen, H., Kreissl, F., Kvashin, A., Laaksonen, A., Lehtipalo, K., Lima, J., Lovejoy, E. R.,

**Thermodynamics of
sulfuric acid dimer
formation**

A. Kürten et al.

Title Page

Abstract

Introduction

Conclusions

References

Tables

Figures



Back

Close

Full Screen / Esc

Printer-friendly Version

Interactive Discussion



Hutterli, M., Kangasluoma, J., Kirkby, J., Laaksonen, A., Lehtipalo, K., Leiminger, M., Makhmutov, V., Mathot, S., Onnela, A., Petäjä, T., Praplan, A. P., Riccobono, F., Rissanen, M. P., Rondo, L., Schobesberger, S., Seinfeld, J. H., Steiner, G., Tomé, A., Tröstl, J., Winkler, P. M., Williamson, C., Wimmer, D., Ye, P., Baltensperger, U., Carslaw, K. S., Kulmala, M., Worsnop, D. R., and Curtius, J.: Neutral molecular cluster formation of sulfuric acid-dimethylamine observed in real-time under atmospheric conditions, *P. Natl. Acad. Sci. USA*, 111, 15019–15024, doi:10.1073/pnas.1404853111, 2014.

Kurtén, T., Torpo, L., Ding, C.-G., Vehkamäki, H., Sundberg, M. R., Laasonen, K., and Kulmala, M.: A density functional study on water-sulfuric acid-ammonia clusters and implications for atmospheric cluster formation, *J. Geophys. Res.*, 112, D04210, doi:10.1029/2006JD007391, 2007.

Lee, S.-H., Reeves, J. M., Wilson, J. C., Hunton, D. E., Viggiano, A. A., Miller, T. M., Ballenthin, J. O., and Lait, L. R.: Particle formation by ion nucleation in the upper troposphere and lower stratosphere, *Science*, 301, 1886–1889, doi:10.1126/science.1087236, 2003.

Lovejoy, E. R. and Curtius, J.: Cluster ion thermal decomposition (II): master equation modeling in the low-pressure limit and fall-off regions, Bond energies for $\text{HSO}_4^-(\text{H}_2\text{SO}_4)_x(\text{HNO}_3)_y$, *J. Phys. Chem. A*, 105, 10874–10883, 2001.

Lovejoy, E. R., Curtius, J., and Froyd, K. D.: Atmospheric ion-induced nucleation of sulfuric acid and water, *J. Geophys. Res.*, 109, D08204, doi:10.1029/2003JD004460, 2004.

Mauldin, R. L., Tanner, D. J., Heath, J. A., Huebert, B. J., and Eisele, F. L.: Observations of H_2SO_4 and MSA during PEM-Tropics-A, *J. Geophys. Res.*, 104, 5801–5816, 1999.

McMurry, P. H.: Photochemical aerosol formation from SO_2 : a theoretical analysis of smog chamber data, *J. Colloid Interf. Sci.*, 78, 513–527, 1980.

Murphy, D. M. and Koop, T.: Review of the vapour pressures of ice and supercooled water for atmospheric applications, *Q. J. Roy. Meteor. Soc.*, 131, 1539–1565, 2005.

Norman, M., Hansel, A., and Wisthaler, A.: O_2^+ as reagent ion in the PTR-MS instrument: detection of gas-phase ammonia, *Int. J. Mass Spectrom.*, 265, 382–387, 2007.

Ortega, I. K., Kupiainen, O., Kurtén, T., Olenius, T., Wilkman, O., McGrath, M. J., Loukonen, V., and Vehkamäki, H.: From quantum chemical formation free energies to evaporation rates, *Atmos. Chem. Phys.*, 12, 225–235, doi:10.5194/acp-12-225-2012, 2012.

Ortega, I. K., Olenius, T., Kupiainen-Määttä, O., Loukonen, V., Kurtén, T., and Vehkamäki, H.: Electrical charging changes the composition of sulfuric acid-ammonia/dimethylamine clusters, *Atmos. Chem. Phys.*, 14, 7995–8007, doi:10.5194/acp-14-7995-2014, 2014.

**Thermodynamics of
sulfuric acid dimer
formation**

A. Kürten et al.

Title Page

Abstract

Introduction

Conclusions

References

Tables

Figures



Back

Close

Full Screen / Esc

Printer-friendly Version

Interactive Discussion



- Paasonen, P., Olenius, T., Kupiainen, O., Kurtén, T., Petäjä, T., Birmili, W., Hamed, A., Hu, M., Huey, L. G., Plass-Duelmer, C., Smith, J. N., Wiedensohler, A., Loukonen, V., McGrath, M. J., Ortega, I. K., Laaksonen, A., Vehkamäki, H., Kerminen, V.-M., and Kulmala, M.: On the formation of sulphuric acid – amine clusters in varying atmospheric conditions and its influence on atmospheric new particle formation, *Atmos. Chem. Phys.*, 12, 9113–9133, doi:10.5194/acp-12-9113-2012, 2012.
- Petäjä, T., Sipilä, M., Paasonen, P., Nieminen, T., Kurtén, T., Ortega, I. K., Stratmann, F., Vehkamäki, H., Berndt, T., and Kulmala, M.: Experimental observation of strongly bound dimers of sulfuric acid: application to nucleation in the atmosphere, *Phys. Rev. Lett.*, 106, 228302-1–228302-4, 2011.
- Praplan, A. P., Bianchi, F., Dommen, J., and Baltensperger, U.: Dimethylamine and ammonia measurements with ion chromatography during the CLOUD4 campaign, *Atmos. Meas. Tech.*, 5, 2161–2167, doi:10.5194/amt-5-2161-2012, 2012.
- Riccobono, F., Schobesberger, S., Scott, C. E., Dommen, J., Ortega, I. K., Rondo, L., Almeida, J., Amorim, A., Bianchi, F., Breitenlechner, M., David, A., Downard, A., Dunne, E. M., Duplissy, J., Ehrhart, S., Flagan, R. C., Franchin, A., Hansel, A., Junninen, H., Kajos, M., Keskinen, H., Kupc, A., Kürten, A., Kvashin, A. N., Laaksonen, A., Lehtipalo, K., Makhmutov, V., Mathot, S., Nieminen, T., Onnela, A., Petäjä, T., Praplan, A. P., Santos, F. D., Schallhart, S., Seinfeld, J. H., Sipilä, M., Spracklen, D. V., Stozhkov, Y., Stratmann, F., Tomé, A., Tsagkogeorgas, G., Vaattovaara, P., Viisanen, Y., Vrtala, A., Wagner, P. E., Weingartner, E., Wex, H., Wimmer, D., Carslaw, K. S., Curtius, J., Donahue, N. M., Kirkby, J., Kulmala, M., Worsnop, D. R., and Baltensperger, U.: Oxidation products of biogenic emissions contribute to nucleation of atmospheric particles, *Science*, 344, 717–721, 2014.
- Rondo, L., Kürten, A., Ehrhart, S., Schobesberger, S., Franchin, A., Junninen, H., Petäjä, T., Sipilä, M., Worsnop, D. R., and Curtius, J.: Effect of ions on the measurement of sulfuric acid in the CLOUD experiment at CERN, *Atmos. Meas. Tech.*, 7, 3849–3859, doi:10.5194/amt-7-3849-2014, 2014.
- Sceats, M. G.: Brownian coagulation in aerosols – the role of long range forces, *J. Colloid Interf. Sci.*, 129, 105–112, 1989.
- Schobesberger, S., Junninen, H., Bianchi, F., Lönn, G., Ehn, M., Lehtipalo, K., Dommen, J., Ehrhart, S., Ortega, I. K., Franchin, A., Nieminen, T., Riccobono, F., Hutterli, M., Duplissy, J., Almeida, J., Amorim, A., Breitenlechner, M., Downard, A. J., Dunne, E. M., Flagan, R. C., Kajos, M., Keskinen, H., Kirkby, J., Kupc, A., Kürten, A., Kurtén, T., Laakso-

**Thermodynamics of
sulfuric acid dimer
formation**

A. Kürten et al.

Title Page

Abstract

Introduction

Conclusions

References

Tables

Figures



Back

Close

Full Screen / Esc

Printer-friendly Version

Interactive Discussion



nen, A., Mathot, S., Onnela, A., Praplan, A. P., Rondo, L., Santos, F. D., Schallhart, S., Schnitzhofer, R., Sipilä, M., Tomé, A., Tsagkogeorgas, G., Vehkamäki, H., Wimmer, D., Baltensperger, U., Carslaw, K. S., Curtius, J., Hansel, A., Petäjä, T., Kulmala, M., Donahue, N. M., and Worsnop, D. R.: Molecular understanding of atmospheric particle formation from sulfuric acid and large oxidized organic molecules, *P. Natl. Acad. Sci. USA*, 110, 17223–17228, doi:10.1073/pnas.1306973110, 2013.

Schobesberger, S., Franchin, A., Bianchi, F., Rondo, L., Duplissy, J., Kürten, A., Ortega, I. K., Metzger, A., Schnitzhofer, R., Almeida, J., Amorim, A., Dommen, J., Dunne, E. M., Ehn, M., Gagné, S., Ickes, L., Junninen, H., Hansel, A., Kerminen, V.-M., Kirkby, J., Kupc, A., Laaksonen, A., Lehtipalo, K., Mathot, S., Onnela, A., Petäjä, T., Riccobono, F., Santos, F. D., Sipilä, M., Tomé, A., Tsagkogeorgas, G., Viisanen, Y., Wagner, P. E., Wimmer, D., Curtius, J., Donahue, N. M., Baltensperger, U., Kulmala, M., and Worsnop, D. R.: On the composition of ammonia–sulfuric-acid ion clusters during aerosol particle formation, *Atmos. Chem. Phys.*, 15, 55–78, doi:10.5194/acp-15-55-2015, 2015.

Torpo, L., Kurtén, T., Vehkamäki, H., Laasonen, K., Sundberg, M. R., and Kulmala, M.: Significance of ammonia in growth of atmospheric nanoclusters, *J. Phys. Chem. A*, 111, 10671–10674, 2007.

Viggiano, A. A., Seeley, J. V., Mundis, P. L., Williamson, J. S., and Morris, R. A.: Rate constants for the reactions of $XO_3^- (H_2O)_n$ ($X = C, HC, \text{ and } N$) and $NO_3^- (HNO_3)_n$ with H_2SO_4 : implications for atmospheric detection of H_2SO_4 , *J. Phys. Chem. A*, 101, 8275–8278, 1997.

Voigtländer, J., Duplissy, J., Rondo, L., Kürten, A., and Stratmann, F.: Numerical simulations of mixing conditions and aerosol dynamics in the CERN CLOUD chamber, *Atmos. Chem. Phys.*, 12, 2205–2214, doi:10.5194/acp-12-2205-2012, 2012.

Weber, R. J., McMurry, P. H., Eisele, F. L., and Tanner, D. J.: Measurement of expected nucleation precursor species and 3–500-nm diameter particles at Mauna Loa observatory, Hawaii, *J. Atmos. Sci.*, 52, 2242–2257, 1995.

Weber, R., McMurry, P. H., Mauldin, L., Tanner, D. J., Eisele, F. L., Brechtel, F. J., Kreidenweis, S. M., Kok, G., Schillawski, R. D., and Baumgardner, D.: A study of new particle formation and growth involving biogenic and trace gas species measured during ACE 1, *J. Geophys. Res.*, 103, 16385–16396, 1998.

Weigel, R., Borrmann, S., Kazil, J., Minikin, A., Stohl, A., Wilson, J. C., Reeves, J. M., Kunkel, D., de Reus, M., Frey, W., Lovejoy, E. R., Volk, C. M., Viciani, S., D'Amato, F., Schiller, C., Peter, T., Schlager, H., Cairo, F., Law, K. S., Shur, G. N., Belyaev, G. V., and Curtius, J.: In situ

observations of new particle formation in the tropical upper troposphere: the role of clouds and the nucleation mechanism, *Atmos. Chem. Phys.*, 11, 9983–10010, doi:10.5194/acp-11-9983-2011, 2011.

5 Zhang, R., Khalizov, A., Wang, L., Hu, M., and Xu, W.: Nucleation and growth of nanoparticles in the atmosphere, *Chem. Rev.*, 112, 1957–2011, 2012.

Zhao, J., Eisele, F. L., Titcombe, M., Kuang, C., and McMurry, P. H.: Chemical ionization mass spectrometric measurements of atmospheric neutral clusters using the cluster-CIMS, *J. Geophys. Res.*, 115, D08205, doi:10.1029/2009JD012606, 2010.

10 Zollner, J. H., Glasoe, W. A., Panta, B., Carlson, K. K., McMurry, P. H., and Hanson, D. R.: Sulfuric acid nucleation: power dependencies, variation with relative humidity, and effect of bases, *Atmos. Chem. Phys.*, 12, 4399–4411, doi:10.5194/acp-12-4399-2012, 2012.

Thermodynamics of sulfuric acid dimer formation

A. Kürten et al.

Title Page

Abstract

Introduction

Conclusions

References

Tables

Figures



Back

Close

Full Screen / Esc

Printer-friendly Version

Interactive Discussion



Thermodynamics of
sulfuric acid dimer
formation

A. Kürten et al.

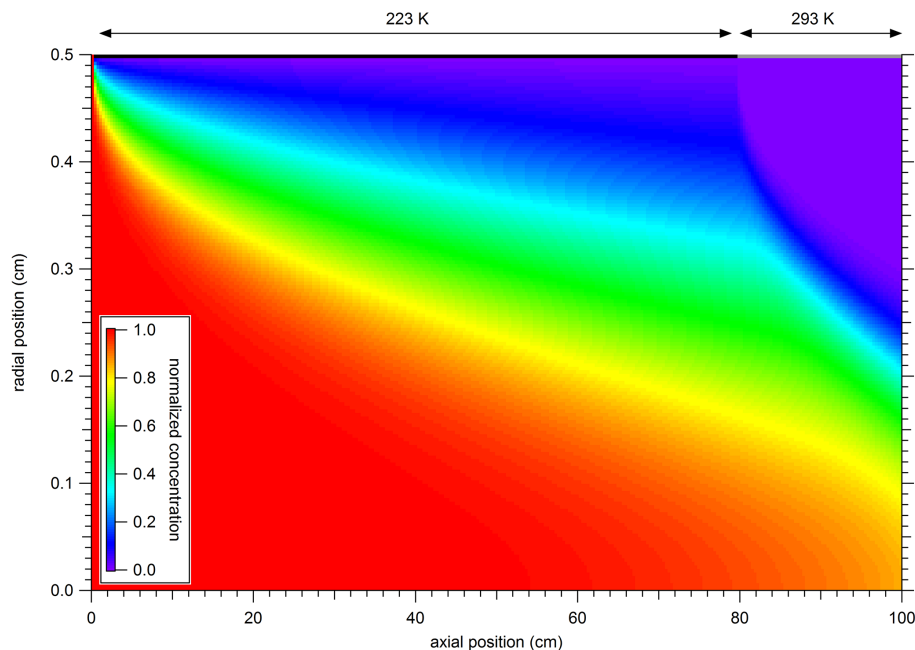


Figure 1. Simulated transmission of dimers through the CIMS sampling line at a temperature of 223 K for the incoming air. The temperature of the sampling line is fixed to 223 K for the first 80 cm (black color at top axis) and to 293 K for the last 20 cm (grey color at top axis). Wall loss is the dominant loss process over the first 80 cm, whereas evaporation is an additional loss process for the last 20 cm. The overall transmission (diffusion loss and evaporation) is 22.8% at a flow rate of 7.6 L min^{-1} , while it is 47.5% when evaporation is neglected (diffusion loss only). See text for details.

[Title Page](#)[Abstract](#)[Introduction](#)[Conclusions](#)[References](#)[Tables](#)[Figures](#)[◀](#)[▶](#)[◀](#)[▶](#)[Back](#)[Close](#)[Full Screen / Esc](#)[Printer-friendly Version](#)[Interactive Discussion](#)

Thermodynamics of sulfuric acid dimer formation

A. Kürten et al.

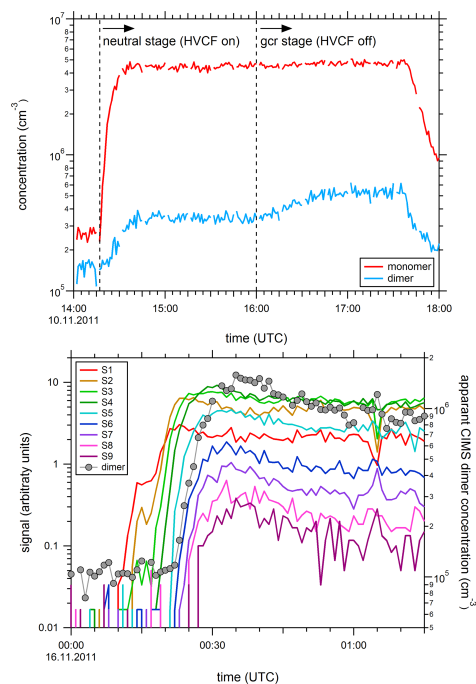


Figure 2. Upper panel: observed ion effect on CIMS sulfuric acid dimer (m/z 195) measurements at 223 K. The first part of the experiment is under neutral conditions, the second part is a GCR run with ions present in the chamber. The increase in the dimer signal during the GCR stage is due to ions detected by the CIMS and not due to neutral dimers. Lower panel: comparison between the API-TOF signals and the CIMS dimer measurements for a different ion-induced experiment at 223 K. The ion clusters (S6, i.e. $\text{HSO}_4^-(\text{H}_2\text{SO}_4)_5$ and larger) show a clear correlation with the apparent dimer signal, which indicates that fragmented cluster ions contribute to the CIMS dimer measurement (Pearson's correlation coefficient between dimer and S6 is 0.93).

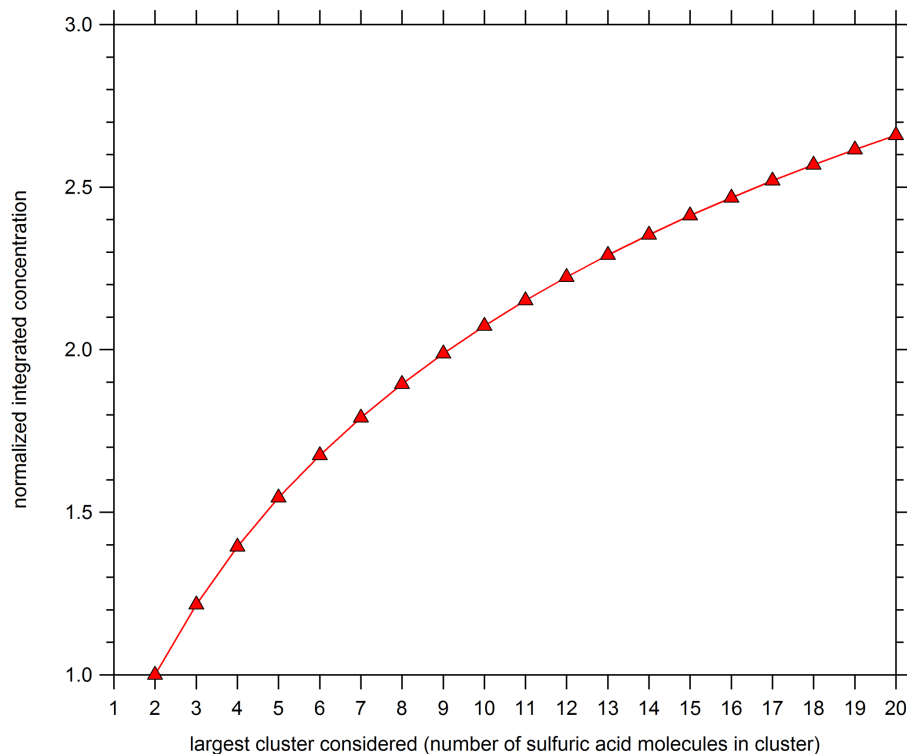


Figure 3. Simulated integrated cluster concentrations at 223K and 20% RH ($k_{2,e} = 5.1 \text{ s}^{-1}$ and $k_{3,e} = 0.056 \text{ s}^{-1}$; all larger evaporation rates are zero). The cluster concentrations are integrated up to a certain number of sulfuric acid molecules in a cluster starting with the dimer concentration. The values on the x axis indicate the number of sulfuric acid molecules in the largest cluster considered in the integration. All concentrations are normalized by the dimer concentration (at $2.0 \times 10^7 \text{ cm}^{-3}$ monomer concentration).

Thermodynamics of sulfuric acid dimer formation

A. Kürten et al.

Title Page	
Abstract	Introduction
Conclusions	References
Tables	Figures
◀	▶
◀	▶
Back	Close
Full Screen / Esc	
Printer-friendly Version	
Interactive Discussion	



Thermodynamics of sulfuric acid dimer formation

A. Kürten et al.

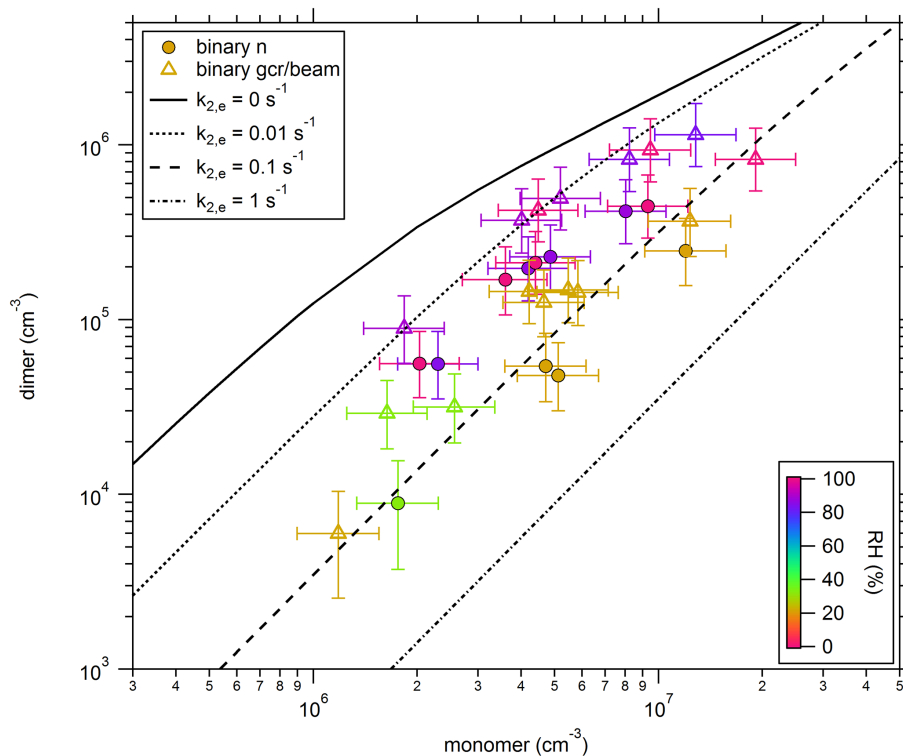


Figure 4. Sulfuric acid dimer concentration as a function of the monomer concentration at 208 K for binary conditions. The full circles are from neutral experiments obtained at steady-state and the open triangles from ion-induced experiments. The black lines indicate the modeled dimer concentration for a given dimer evaporation rate with all other cluster evaporation rates set to zero. The color code indicates the relative humidity.

[Title Page](#)
[Abstract](#)
[Introduction](#)
[Conclusions](#)
[References](#)
[Tables](#)
[Figures](#)
[Back](#)
[Close](#)
[Full Screen / Esc](#)
[Printer-friendly Version](#)
[Interactive Discussion](#)

Thermodynamics of sulfuric acid dimer formation

A. Kürten et al.

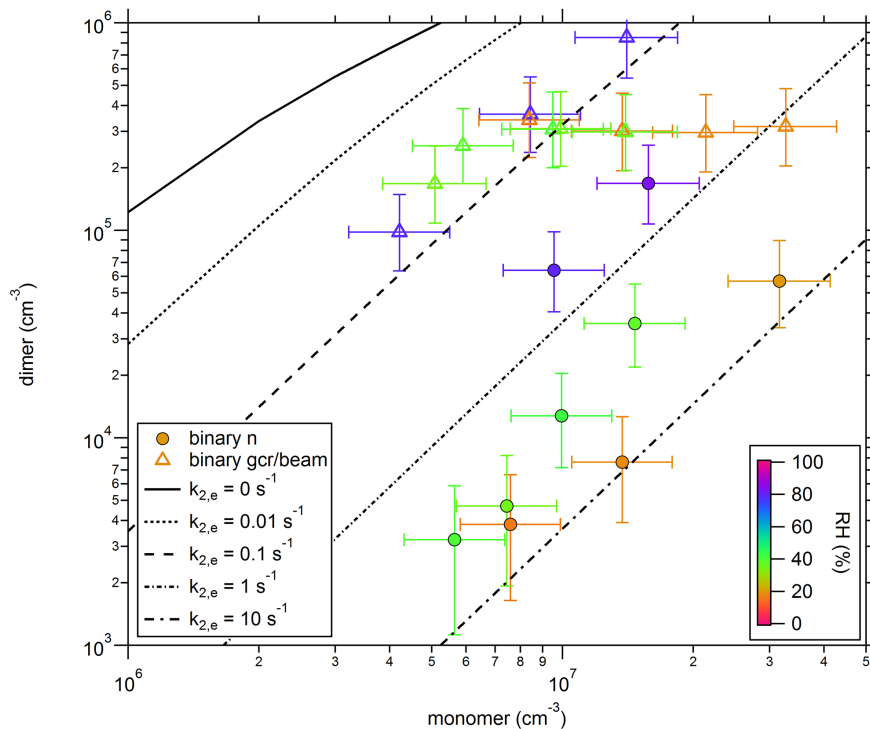


Figure 5. Same as Fig. 4 but for a temperature of 223 K.

Title Page

Abstract

Introduction

Conclusions

References

Tables

Figures

◀

▶

◀

▶

Back

Close

Full Screen / Esc

Printer-friendly Version

Interactive Discussion



Thermodynamics of sulfuric acid dimer formation

A. Kürten et al.

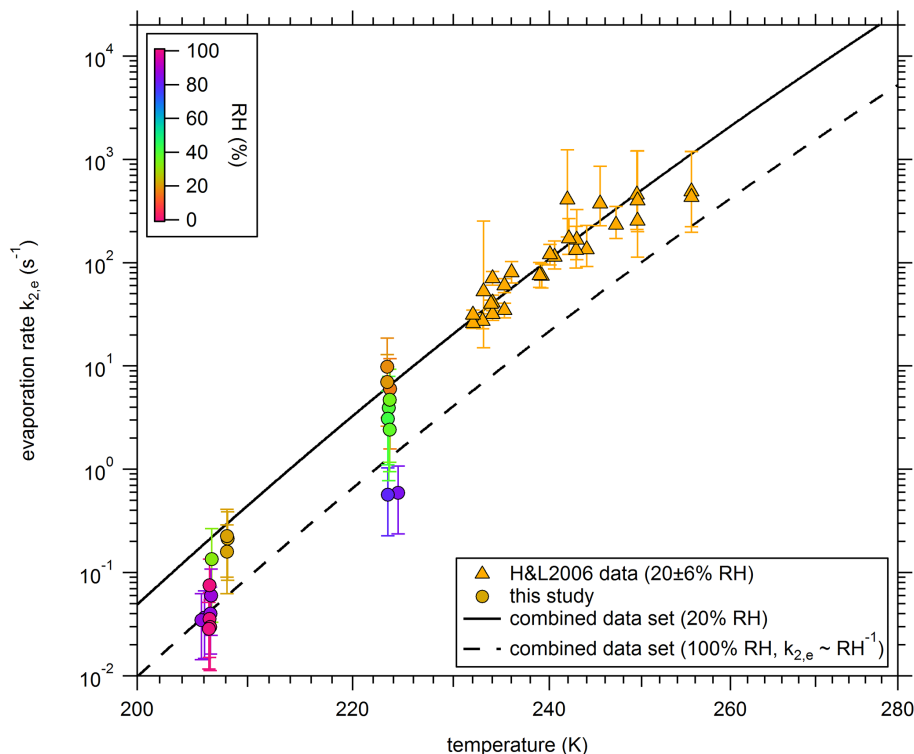


Figure 6. Comparison of the sulfuric acid dimer evaporation rates from this study (circles) and from the literature (triangles, see Hanson and Lovejoy, 2006) as a function of temperature. The color code indicates the relative humidity during the experiments. The solid line represents a best fit through the data with the thermodynamic properties $dH = -18.6 \pm 1.3 \text{ kcal mol}^{-1}$ and $dS = -40.7 \pm 5.5 \text{ cal mol}^{-1} \text{ K}^{-1}$ at 20% RH. The dashed line shows the dimer evaporation rates for a relative humidity of 100% assuming a power dependency of $k_{2,e} \sim \text{RH}^{-1}$.

Title Page

Abstract

Introduction

Conclusions

References

Tables

Figures



Back

Close

Full Screen / Esc

Printer-friendly Version

Interactive Discussion



Thermodynamics of sulfuric acid dimer formation

A. Kürten et al.

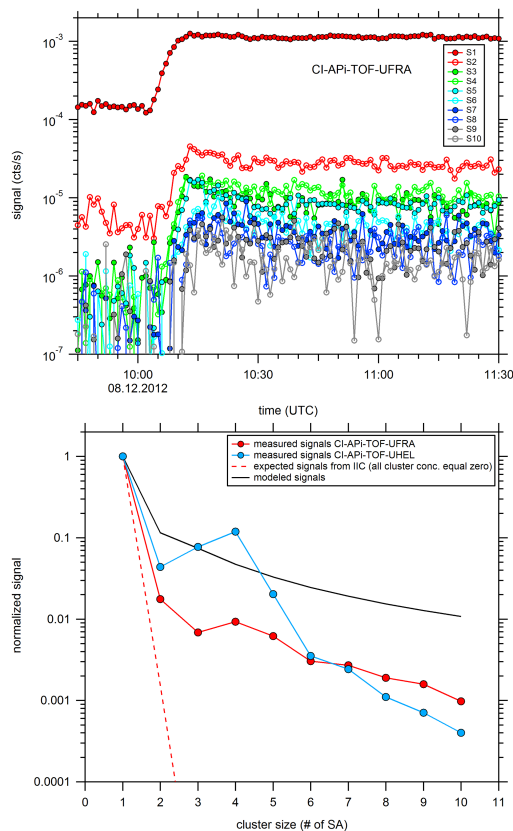


Figure 7. Cluster measurements for the binary system at 206 K and a RH close to 100 % over ice measured with two CI-API-TOFs (UFRAs and UHEL instruments). The upper panel shows the monomer (S1) and the cluster signals (Si, $i \geq 2$) normalized by the nitrate ion signals as a function of time (1 min time resolution) for the CI-API-TOF-UFRAs. The lower panel shows the measured steady-state signals as well as expected signals using different assumptions as function of the cluster size. See text for details.

Thermodynamics of sulfuric acid dimer formation

A. Kürten et al.

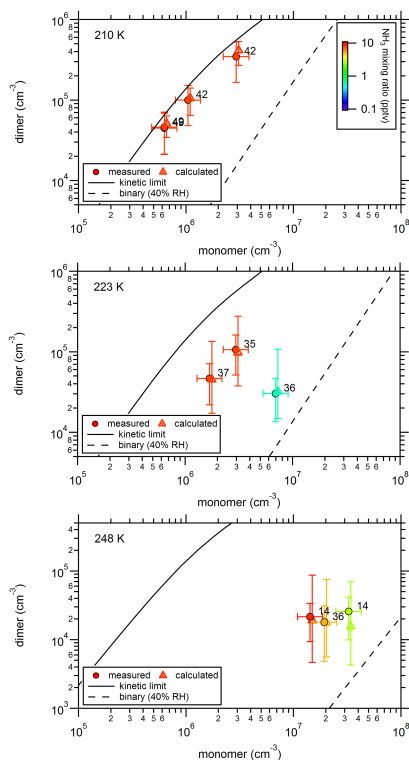


Figure 8. Sulfuric acid dimer concentrations as a function of the sulfuric acid monomer concentration at three different temperatures for the ternary system involving ammonia (ammonia mixing ratio indicated by the color code). The colored circles are the measured concentrations. Lines are from model calculations indicating the expected concentrations for the binary system (dashed line) and the kinetic limit (solid line). The numbers indicate the RH (in %) during the experiment. Open colored triangles are the simulated dimer concentrations using the reaction scheme from Fig. 9. These are slightly offset to the right in order to improve readability.

Title Page

Abstract

Introduction

Conclusions

References

Tables

Figures



Back

Close

Full Screen / Esc

Printer-friendly Version

Interactive Discussion



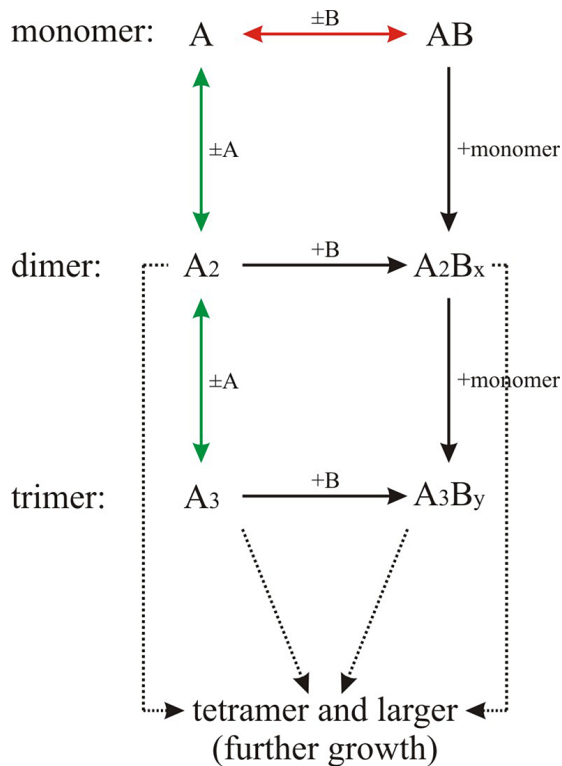


Figure 9. Reaction scheme for the sulfuric acid dimer formation in the ternary system at a low temperature. “A” denotes a sulfuric acid molecule, and “B” an ammonia molecule. “Monomer” is the sum of the concentration of the pure sulfuric acid (A) and the sulfuric acid bound to an ammonia (AB). “Dimer” is the sum of all clusters containing two sulfuric acid molecules ($A_2 + A_2B + A_2B_2$) and the same applies for the “trimer” with three sulfuric acid molecules. The arrows indicate the relevant reactions and whether only collisional growth (single-ended arrow) or growth as well as evaporation (double-ended arrow) are important. Losses due to walls, dilution and coagulation are included in the model but not indicated. See text for details.